CHARACTERIZATION OF THE IRON CENTER IN CYSTEINE DIOXYGENASE

AND KINETIC ANALYSES OF FLAVIN BINDING BY THE

ALKANESULFONATE FLAVIN REDUCTASE

Except where reference is made to the work of others, the work described in this thesis is my own or was done in collaboration with my advisory committee.
This thesis does not include proprietary or classified information.

Honglei Sun

Certificate of Approval:

Douglas C. Goodwin Assistant Professor Chemistry and Biochemistry	Holly R. Ellis. Chair Associate Professor Chemistry and Biochemistry
Evert C. Duin Assistant Professor Chemistry and Biochemistry	Stephen L. McFarland Dean Graduate School

CHARACTERIZATION OF THE IRON CENTER IN CYSTEINE DIOXYGENASE AND KINETIC ANALYSES OF FLAVIN BINDING BY THE ALKANESULFONATE FLAVIN REDUCTASE

Honglei Sun

A Thesis

Submitted to

the Graduate Faculty of

Auburn University

in Partial Fulfillment of the

Requirements for the

Degree of

Master of Science

Auburn, Alabama
December 15, 2006

CHARACTERIZATION OF THE IRON CENTER IN CYSTEINE DIOXYGENASE

AND KINETIC ANALYSES OF FLAVIN BINDING BY THE

ALKANESULFONATE FLAVIN REDUCTASE

Honglei Sun

_____
Signature of Author

_____
Date of Graduation

VITA

Honglei Sun was born in Weifang, Shandong Province, P. R. China, on January 2, 1980. He graduated from Linqu No.1 High School, Shandong Province in June of 1997. From 1997-2001 he studied in Dalian University of Technology with a major of Chemical Engineering. After graduation as a bachelor he attended Guangzhou Energy Conservation Institute for Master Degree from 2001-2003. In fall 2003, he was enrolled by Auburn University in the Department of Chemistry and Biochemistry for a Master's degree.

THESIS ABSTRACT

CHARACTERIZATION OF THE IRON CENTER IN CYSTEINE DIOXYGENASE AND KINETIC ANALYSES OF FLAVIN BINDING BY THE ALKANESULFONATE FLAVIN REDUCTASE

Honglei Sun

Master of Science, December 15, 2006
(B.S. degree, Dalian University of Technology, 2001)

109 Typed Pages

Directed by Holly R. Ellis

Cysteine dioxygenase (CDO) and the flavin reductase, SsuE, are both important proteins in sulfur metabolism. CDO catalyzes cysteine oxidation which is a key step in cysteine metabolism in mammalian systems. SsuE is a flavin reductase found in bacteria that is part of a two-component system involved in sulfur assimilation from alkanesulfonates during sulfur starvation.

Following purification of CDO, two bands at ~23 kDa and ~25 kDa were observed by SDS-PAGE. In addition, purified CDO was shown to lose activity over time. A series of experiments were carried out to characterize the two bands and determine what leads to the activity loss of CDO. Results showed that the two bands had the same molecular weight and amino acid sequence, indicating there was no

apparent difference between the two proteins. Recent studies from our laboratory have shown that a crosslink between Tyr157 and Cys93 in CDO is responsible for the formation of the lower molecular weight band observed on SDS-PAGE. The participation of the iron center and Tyr157 in the formation of this crosslink may lead to the activity loss of purified CDO protein under aerobic conditions. EPR studies of CDO showed that L-cysteine coordinated to the iron center and altered the environment of the active site. In conclusion, the two bands of CDO have similar molecular weights and amino acid composition, and cysteine binding to the active site alters the environment of the iron center. These studies clarify the composition of these two bands and help to further elucidate the mechanism of CDO.

SsuE shares a similar function with the NAD(P)H:flavin reductase (Fre protein) from *E. coli* that belongs to the ferredoxin-$NADP^+$ (FNR) family. Although there is no significant sequence homology between SsuE and other flavin reductases, a conserved motif, $R_{51}XXS_{54}$ found in the FNR family is observed in SsuE. Previous studies have shown this motif plays a key role in the recognition of the isoalloxazine ring and flavin catalysis. Based on the role of this motif in the FNR family, the substitution of Ser54 and Phe52 to Ala in SsuE has been performed by site-directed mutagenesis. Kinetic studies of these two mutant proteins showed that Ser54 is involved in flavin binding and Phe52 is likely involved in SsuE catalysis. The pH profile of SsuE suggests that the optimal activity occurs at a pH above 5.0. Future studies will focus on the detailed kinetic analyses of these putative conserved active site residues in SsuE.

ACKNOWLEDGEMENTS

I would like to firstly thank my advisor, Dr. Holly R. Ellis for her kind support as a knowledgeable professor and a kind mentor. My thesis would not be possible without her support and guidance. Secondly, I want to thank my respectable committee members, Dr. Goodwin and Dr. Duin for their correction and suggestions to my thesis. I also want to thank my lab colleagues, Benlian Gao, Kholis Abdurachim, Russell Carpenter, Erin Imsand Massey, Xuanzhi Zhan and last but not least, I want to thank Auburn University which offered me the chance to study here.

Style Manual Used: Biochmical and Biophysical Research Communications

Computer Software Used: Microsoft Word, Microsoft Excel, ChemDraw, KaleidaGragh

TABLE OF CONTENTS

LIST OF FIGURES AND TABLES

INTRODUCTION TO SULFUR METABOLISM

Sulfur is an essential element in all organisms, which can be assimilated from various sources. For mammalian organisms, the major sulfur sources are methionine (Met) and cysteine (Cys), with Cys as the preferred sulfur source (1). Met is an essential amino acid for mammalian organisms which can only be obtained from the diet while Cys can be synthesized from Met. The major metabolic pathways for these amino acids are shown in Figure 1. Besides their importance in protein synthesis, Met and Cys play important metabolic roles. Met metabolites act as methyl donors in transmethylation reactions and as aminopropyl donors in the synthesis of polyamines. Met is also utilized in the formation of Cys *via* the transmethylation-transsulfuration pathway (Figure 1). Cysteine is a precursor for glutathione (GSH) synthesis, or is converted to pyruvate and sulfite or taurine. Sulfate is required for various sulfation reactions including the sulfation of glycosaminoglycans and the formation of sulfate esters of some drugs (2, 3) Taurine is a conditionally-essential amino acid and plays important roles in mammalian organisms.

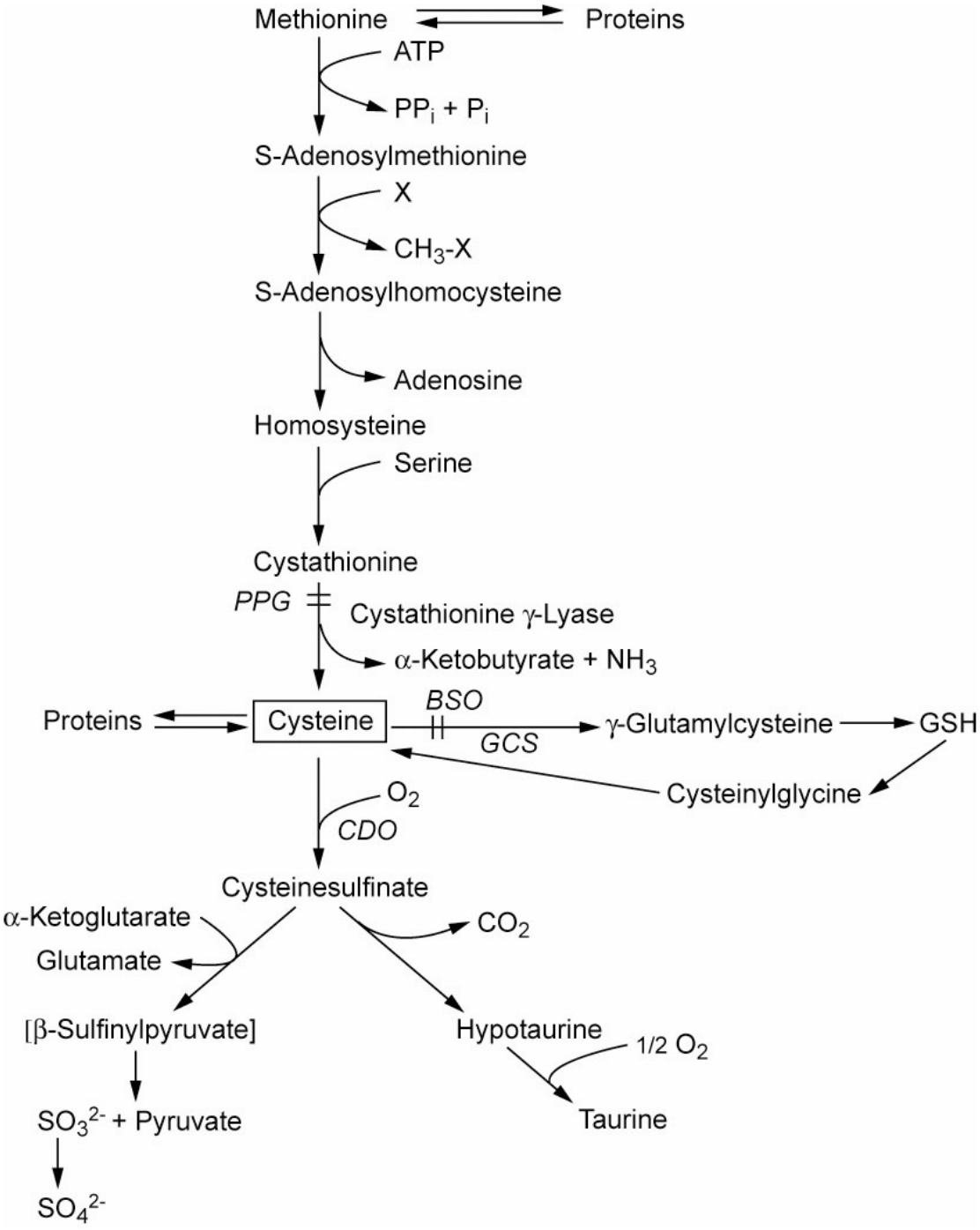

Figure 1. Major pathways of sulfur amino acid metabolism (4).

Cysteine dioxygenase (CDO) catalyzes the rate-limiting step in the pathway that results in the formation of pyruvate and sulfate or taurine (Figure 1). CDO plays important roles in taurine and sulfate synthesis, and maintaining the cysteine pool. Thus, the study of CDO has important physiological significance. Although the three-dimensional crystal structure of CDO has recently been solved (24, 25), there are several structural and mechanistic questions that remain to be determined. First, it is not known how cysteine oxidation is catalyzed by CDO. Second, the iron center has not been characterized. Lastly, CDO resolves as two bands on SDS-PAGE, and the difference between these two forms of CDO has not been elucidated.

Bacteria can assimilate sulfur from different sources other than Cys and Met (Figure 2). Sulfate is the major sulfur source for bacteria. It can be transferred from the environment to the cell, reduced to sulfite and sulfide and then used to synthesize cysteine *via* the cysteine biosynthetic pathway (Figure 2) (1). In the absence of sulfate and Cys, a set of enzymes are induced to utilize organic sulfur sources. For example, *Escherichia coli* can use aliphatic sulfonates as sulfur sources (1). Expression of two gene clusters, *tau*ABCD and *ssu*EADCB, are required for the utilization of sulfonate compounds from the environment. Each of the genes encodes an ATP-binding cassette-type (ABC-type) transport system for the uptake of aliphatic sulfonates and enzymes for desulfonation. TauD is an α-ketoglutarate-dependent dioxygenase enzyme which catalyzes the desulfonation of taurine, whereas. SsuD is a monooxygenase which

catalyzes the desulfonation of aliphatic sulfonates. It requires $FMNH_2$ as its cosubstrate, which is provided by SsuE an NAD(P)H dependent FMN reductase. SsuE, and SsuD together are referred to as the alkanesulfonate monooxygenase system. TauD and SsuD from *E. coli* can complementarily utilize most known organic sulfur sources except cysteate, methanesulfonate, and aromatic sulfonates (1, 5).

SsuE and SsuD form the alkanesulfonate monooxygenase system which is responsible for the utilization of alkanesulfonates. The ability of bacteria to obtain sulfur from sources other than sulfate or Cys assures the cells have an ample supply of this essential element during sulfur starvation. To do so, SsuD requires $FMNH_2$ as the cosubstrate to desulfonate the alkanesulfonate substrates. While free $FMNH_2$ is easily oxidized aerobically, the role of SsuE is to reduce the oxidized FMN for transfer to SsuD. Previous studies have shown that oxidized FMN has a higher binding affinity for SsuE, while $FMNH_2$ has a higher binding affinity for SsuD (32). Interestingly, an alignment search of SsuE with other flavin reductases revealed a conserved amino acid sequence, RXXS. This sequence was previously shown to be involved in flavin binding and catalysis. A focus of this project is to identify the amino acids which are responsible for FMN binding by SsuE.

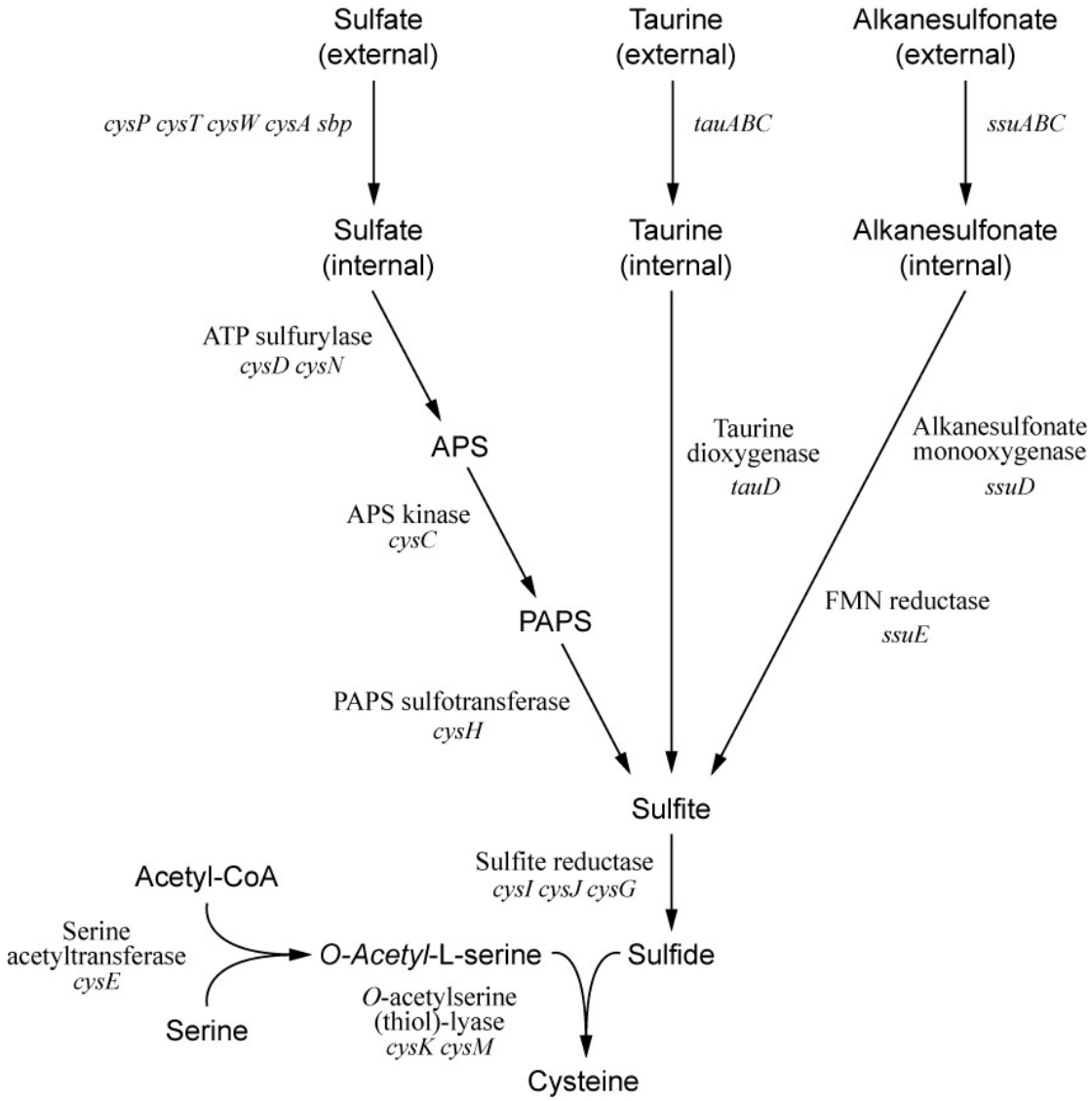

Figure 2. Cysteine biosynthetic pathway from sulfate and alkanesulfonates in *E. coli* (1).

CHAPTER ONE

LITERATURE REVIEW OF CYSTEINE DIOXYGENASE

1.1 Cysteine dioxygenase in cysteine metabolism

Cysteine dioxygenase (CDO) and cysteinesulfinate decarboxylase (CSD) are two key enzymes involved in the conversion of cysteine to taurine (Figure 1.1). CDO catalyzes the conversion of cysteine to cysteinesulfinate or cysteine sulfinic acid (CSA), which is the initial and rate-limiting step for sulfate or taurine biosynthesis (7). CSD decarboxylates CSA to form hypotaurine which is further oxidized to taurine.

CDO has a profound impact on mammalian health by maintaining the cysteine pool and increasing the levels of important metabolites such as taurine. Cysteine at high levels is toxic to cells and readily forms cystine which is poorly soluble. High levels of cysteine have been connected to neurological disorders such as motor neuron, Alzheimer's, and Parkinson's diseases. It also has been shown that cysteine can enhance the toxicity of glutamate which causes excitotoxic behavior.

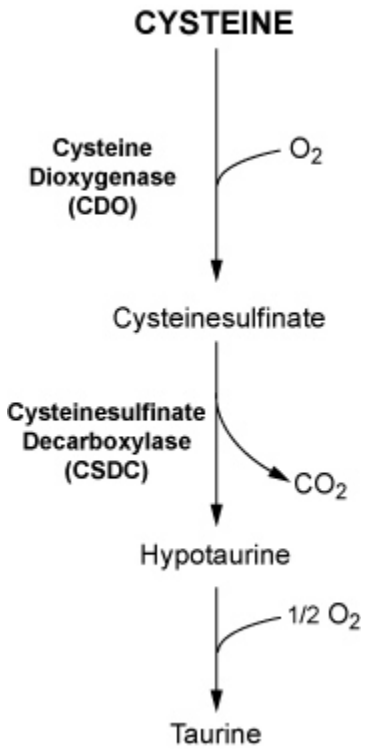

Figure 1.1. Metabolic pathway of cysteine to taurine in mammalian tissues (2).

Taurine has been shown to be essential in various physiological processes (8). Taurine is a conditionally-essential amino acid and is the second most abundant amino acid in the central nervous system. Metabolic roles of taurine include: solubilization of dietary fats, detoxification, membrane stabilization, osmoregulation, and modulation of cellular calcium levels. Taurine conjugation to bile acids has a significant effect on the solubility of cholesterol, and administration of taurine has been shown to reduce serum cholesterol levels in humans. Taurine also functions as a neurotransmitter and plays a key role in stabilizing mammalian skeletal muscle membrane. Additionally, taurine is the most abundant amino acid in mammalian heart tissue. Taurine is able to protect the heart from the adverse effects of either excessive or inadequate calcium, and taurine depletion can result in the deposition of lipids on the arterial wall leading to the development of atherosclerosis.

1.2 Characterization of cysteine dioxygenase

Cysteine dioxygenase was first purified to homogeneity from rat liver by Yamaguchi et al. (9). It was shown to be an iron-containing protein, with a monomeric molecular weight of 23.0 kDa. CDO lost its activity aerobically following purification, but preincubation before activity assay with L-cysteine under anaerobic conditions led to enzyme reactivation. However, CDO so activated was unstable and was rapidly

inactivated during the aerobic assay. A protective protein, protein A, was isolated by the same research group and shown to prevent CDO oxidation. Protein A did not participate in the catalytic reaction because it did not change the K_m value or the initial reaction velocity (9). However, protein A was never characterized. The CDO protein contained 0.8 atoms of iron per monomer. Apo CDO (EDTA was the metal chelating agent) did not possess any activity and supplying extra Fe^{2+} to purified CDO enhanced the activity 2-3 fold, indicating the metal was essential for catalysis.

Rat liver CDO has been cloned and expressed with a histidine tag in *Escherichia coli*, and an active form of CDO has been purified (3, 15). The catalytic activity of CDO was not altered in the presence or absence of the His tag. The recombinant CDO was highly specific for L-cysteine and showed a dependence on Fe^{2+} similar to CDO purified directly from rat liver. The protein was catalytically active even without protein A and was not deactivated by oxygen. Notably, only 10% of the CDO protein contained iron which was significantly lower than previously reported.

1.3 Regulation of CDO

The intracellular free cysteine levels are tightly regulated in mammalian liver within a narrow concentration range. The liver must maintain cysteine levels for the synthesis of proteins and metabolites synthesized from cysteine. Meanwhile, cysteine concentrations must be kept below specific levels because excess cyteine has been shown to be toxic. CDO being the key enzyme in cysteine metabolism plays a central role in controlling cellular or cysteine concentrations in mammalian systems. Thus CDO activity should be regulated by the cell.

The activity of an enzyme can be regulated through a wide range of mechanisms (10, 47). One important way is to control the enzyme availability. The amount of a given enzyme in a cell is determined by both its rate of synthesis and degradation. The rate of enzyme synthesis depends on the cell's need which is controlled by transcriptional, translational, or post-translational regulation. Besides controlling the concentration of enzyme, there are different ways to regulate the enzyme activity. Allosteric enzymes function through allosteric modulators or allosteric effectors. The enzymes other than allosteric ones are regulated by reversible covalent modification such as phosphorylation, adenylylation, uridylylation, ADP-ribosylation, and methylation. In metabolic systems there are at least two other mechanisms of enzyme regulation. Some enzymes are stimulated or inhibited by separate regulatory proteins, and some enzymes are regulated

by irreversible proteolytic cleavage of the enzyme precursor. In some metalloproteins, the enzymes can be activated by reduction of the active-site metal. This reduction can be done by cofactors like FMN or other coenzymes.

CDO activity has a direct dependence on protein obtained from the diet. Higher levels of CDO protein and activity have been observed in liver from rats fed methionine or protein supplemented diets compared to rats fed with basal levels of protein (2). There has been no report that CDO is an allosteric protein, and it appears the activity of CDO is regulated mainly by changes in enzyme concentration. The lack of an apparent increase in CDO mRNA concentrations makes it clear that the regulation of CDO is posttranscriptional. This mode of regulation differs from other key enzymes involved in cysteine metabolism: gamma glutamylcysteine synthetase (GCS) is regulated by pre/posttranslational mechanisms and cysteinesulfinate decarboxylase (CSD) is regulated by translational control (4).

Cysteine has a direct impact on the regulation of CDO activity. CDO-ubiquitin conjugates have been observed in hepatic cells cultured in cysteine-deficient medium and these conjugates are not found in cells cultured in cysteine-supplemented medium (11). Also, inhibitors of the 26S proteasome blocked CDO degradation in cysteine-deficient medium. These results suggest that the ubiquitin-proteasome system is responsible for the

regulation of CDO concentration in liver (11, 12).

Eukaryotic cells contain a multisubunit complex called the 26S proteasome which is responsible for the hydrolysis of most short-lived or regulatory proteins (13). Protein degradation by proteasomes requires ATP and the prior addition of a polyubiquitin chain. Three proteins, E1, E2, and E3, are required to add the ubiquitin chain to the protein to be targeted for degradation. E1 is the ubiquitin-activating enzyme. Ubiquitin is then transferred to E2, the ubiquitin-carrier protein. E3 transfers the activated ubiquitin from E2 to a Lys ϵ-amino group of the previously bound protein, thereby forming an isopeptide bond. E3 plays a central role in recognizing and selecting proteins for degradation.

As mentioned, the presence of cysteine blocks the ubiquitination of CDO, and thus, prevents CDO from proteasomal degradation. Interestingly, cysteamine, which is neither a substrate nor an inhibitor of CDO, has almost the same ability as cysteine to block the ubiquitination of CDO, suggesting that binding of cysteine to the active site is not necessary for blocking CDO ubiquitination (11). How cysteine affects the recognition of CDO by E3 is still unknown.

1.4 Isoforms of cysteine dioxygenase

Multiple forms of CDO (~23.0 kDa, ~25.0 kDa, and 68.0 kDa) have been reported for recombinant and native CDO (15). Does CDO have more than one isoform? The calculated molecular weight of rat CDO from the amino acid sequence is 23.0 kDa, however, conflicting results were obtained for CDO protein purified from rat liver and the recombinant protein expressed in *E. coli* (14). It was first postulated that rat CDO exists in both NAD^+-dependent and NAD^+-independent forms (8). The NAD^+-independent form was found only in liver while the NAD^+-dependent form was found in liver and extrahepatic tissues. Parsons and coworkers have reported a 68.0 kDa CDO from human tissue by immunohistochemistry and Western blotting with anti-CDO antibodies (44). They concluded it was the physiological form of CDO bound to itself or protein A. They also used CDO type II to refer to this putative 68.0 kDa form of CDO.

Recently, research has shown that the purified CDO from rat liver resolves as two bands on SDS-PAGE (2, 15). In one of these reports, the CDO protein was purified with an N-terminal His tag from *E. coli* and was separated by SDS-PAGE (15). Two bands were also observed with apparent molecular weights of ~25.0 kDa and ~23.0 kDa. The 25.0 kDa band was always observed and the 23.0 kDa protein was frequently observed in samples that had high concentrations of CDO. Mass spectrometry of His-tagged CDO yielded two peaks with molecular weights of 24.1 kDa and 24.3 kDa. Anion exchange

FPLC of these two bands resulted in the identification of two peaks (Figure 1.2) (15). Interestingly the first peak contained CDO which had 7.5 times as much as activity as the CDO in the second peak. The first peak yielded two bands at ~23.0 and ~25.0 kDa on SDS-PAGE while the second peak yielded one band at ~23.0 kDa. The difference between the two bands was thought to be caused by an SDS-PAGE artifact which led to a conversion from the 25.0 kDa to the 23.0 kDa form of CDO. Rat CDO protein (lacking a His tag) was also expressed and purified in *E. coli* by our group. Amino acid sequence analysis of these two bands showed that they were identical in sequence.

In conclusion, the two bands identified by SDS-PAGE did not show any difference in molecular weight and the upper molecular weight band had higher activity than the lower band. Why CDO resolved as two bands on SDS-PAGE, and what caused the activity difference between them will be reported herein.

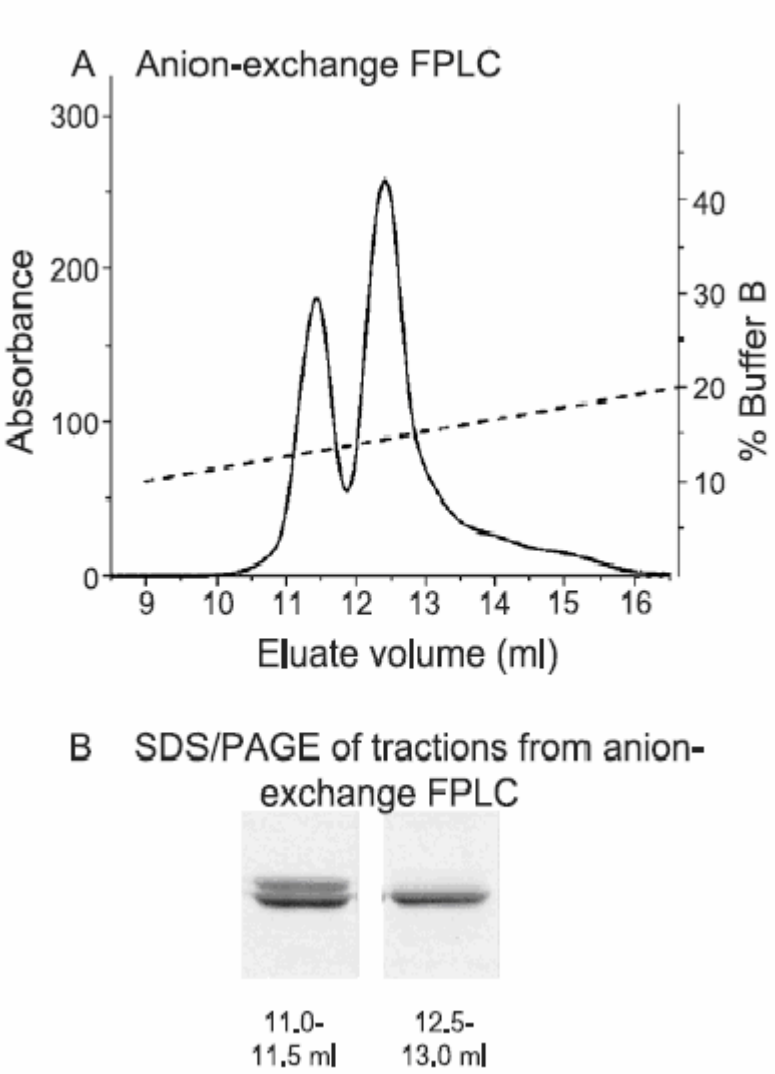

Figure 1.2. Two bands of CDO. **A** Anion-exchange FPLC of r-his$_6$-CDO on a MonoQ HR5/5 column (Amersham Bioscience) using a NaCl gradient; Buffer B contained 1 M NaCl. **B** SDS/PAGE of fractions from peak 1 (11.0-11.5 mL) and peak 2 (12.5-13.0 mL) obtained by anion-exchange FPLC of r-his$_6$-CDO.

1.5 Mechanisms involved in cysteine dioxygenase catalysis

1.5.1 Cysteine oxidase is a dioxygenase

Based on the apparent dependence of reduced pyridine nucleotide in the cysteine aerobic conversion reaction, it was first postulated that CDO might act as a mixed-function monooxygenase, which means CDO would transfer one oxygen atom two times to convert cysteine to cysteine sulfinic acid (CSA) (16). To determine the reaction catalyzed by CDO, $^{18}O_2$ and $H_2{}^{18}O$- $H_2{}^{16}O$ studies were performed (17). Cysteine sulfinic acid was separated from the reaction mixtures and mass spectrometric analysis of CSA showed that both oxygen atoms originated from molecular O_2. There was no oxygen incorporation from water which indicates that the conversion of cysteine to CSA does not occur through a dehydrogenation reaction. Chromatographic separation of the enzyme followed by electro-focusing gave single, symmetrical peaks which suggested that a single protein catalyzed a dioxygenase or mixed-function monooxygenase reaction. The dioxygenase and mixed-function monooxygenase reactions can be distinguished from one another by the requirement for cosubstrates in the reaction. In a mixed-function monooxygenase reaction, one of the two atoms of O_2 enters the substrate, while the other is used to oxidize a cosubstrate (18). There was no absolute dependence on added reduced pyridine nucleotide, and Fe^{+2} was not a likely cosubstrate for cysteine oxygenase. Based on these results, it was concluded that cysteine oxygenase is a dioxygenase

protein.

1.5.2 Role of the Fe^{2+} center in CDO

CDO contains a mononuclear nonheme iron that is essential for the activity of CDO. The apo CDO protein does not possess any activity and the addition of Fe^{2+} can enhance the activity by 2-3 fold.

Many mononuclear nonheme iron proteins share a common structural motif, referred to as the 2-His-1-carboxylate facial triad, that is involved in the activation of dioxygen (19, 20). The iron center is invariably coordinated by two His and one Asp or Glu, constituting one face of an octahedron. The three remaining sites on the opposite face of the octahedron are reserved for exogenous ligands (19). When the enzyme is at rest, these sites are occupied by solvent molecules but can accommodate both substrate and molecular oxygen. As shown for deacetoxycephalosporin C synthetase (DAOCS), at the start of the catalytic process Fe^{2+} is hexa-coordinate and relatively unreactive to O_2 (Figure 1.3). Subsequent substrate and/or cofactor replacement of water molecules makes the iron center penta-coordinate and promotes the coupling between the reduction of O_2 and the oxidation of substrate. This motif allows the iron center to activate both substrate and O_2 and brings them into close proximity for catalysis (19, 20, 21).

Que et al. proposed a mechanism for the extradiol-cleaving dioxygenase enzymes

based on structural and spectroscopic data. (19) (Figure 1.4) The resting state of the enzyme is penta-coordinated with a square pyramidal geometry (Figure 1.4A). The substrate (a catechol in this example) displaces one water molecule and one hydroxide group leaving the opposite site of the Glu ligand open (Figure 1.4B). This displacement is expected to result in a decrease in the redox potential of the iron center that primes it to react with O_2 resulting in the enzyme-substrate-O_2 ternary complex (Figure 1.4C). This arrangement places the substrate and O_2 into a proper orientation for catalysis. Once O_2 binds to the Fe^{2+} center, one electron is transferred from Fe^{2+} to O_2 with the formation of a Fe^{3+}-superoxide complex; a second electron is transferred from substrate to Fe^{3+} (Figure 1.4C, D). Nucleophilic attack of the superoxide on the aromatic ring results in the formation of an alkylperoxo intermediate which undergoes a Criegee rearrangement and then is hydrolyzed to generate the final product (Figure 1.4E, F).

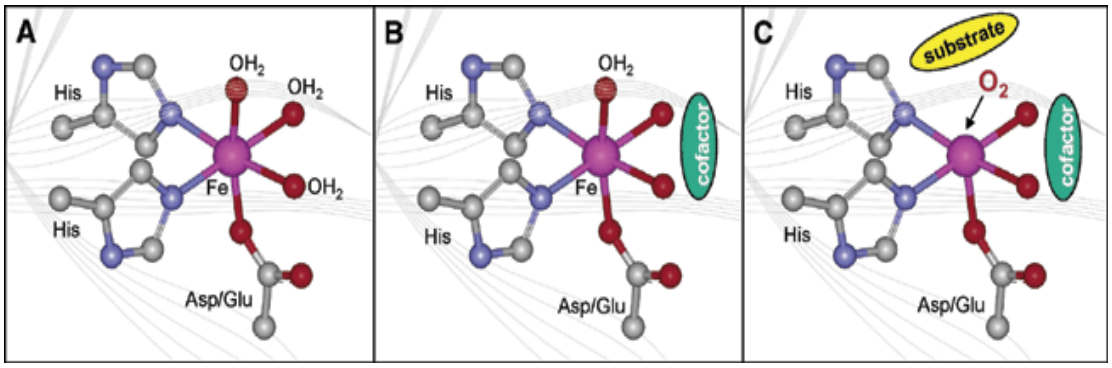

Figure 1.3. Mechanism for dioxygen activation proposed by Solomon for nonheme iron(II) enzymes with a 2-His-1-carboxylate facial triad motif, as exemplified by the active site of DAOCS (1RXF.pdb) (21).

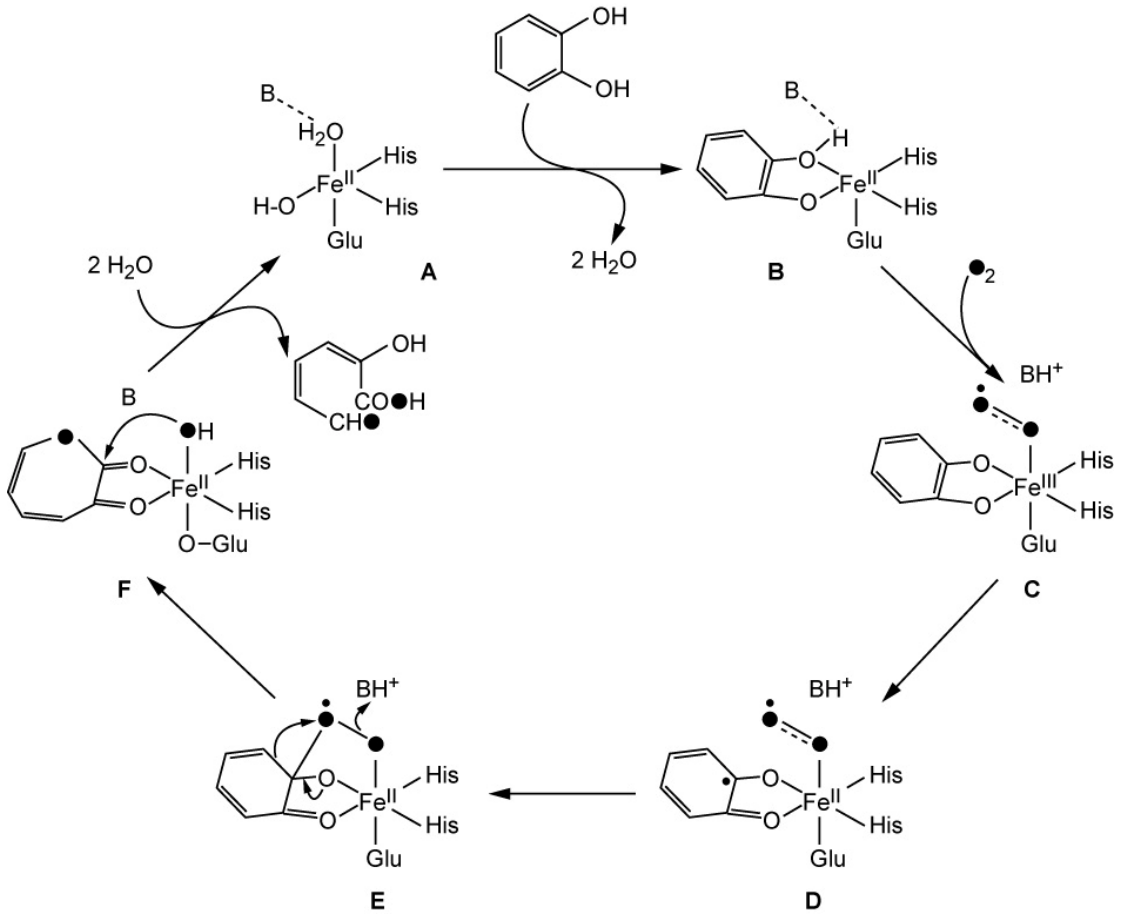

Figure 1.4. Proposed mechanism for the extradiol-cleaving catechol dioxygenases (19).

CDO likely belongs to the intramolecular dioxygenase group, which includes extradiol dioxygenase (22). The extradiol-cleaving enzymes typically follow an ordered mechanism. The substrate binds to the enzyme prior to O_2 activation. Thus the coordination of the substrate may serve as a trigger that significantly increases the affinity of the iron center for O_2. However, the mechanism for O_2 activation by CDO is currently not known.

Recently, the first three-dimensional crystal structure of CDO from *Mus musculus* has been solved to 1.75Å resolution (23). Three His ligands (His86, His88, His140) coordinate the iron in CDO. Additionally, a covalent cross-link between Tyr157 and Cys93 residues was observed. Other conserved active site residues are Tyr58, Arg60, Trp77, Gly100, and His155. According to the observed structural features of the active site, a plausible reaction mechanism was proposed which followed the paradigm for extradiol dioxygenases (Figure 1.5).

The resting enzyme is proposed to be Fe(II) (Figure 1.5 A). Cys coordinates the iron center in a chelating binding through its sulfur and nitrogen atoms (Figure 1.5 B). The binding of Cys may place the sulfur trans to His140. This orientation distinguishes this axis from others in terms of bonding and electron transfer. The region of the active site trans to His86 is hydrophobic and is suitable for O_2 binding. After O_2 coordination, a ternary Fe(III)-superoxo complex is formed (Figure 1.5 C). As a consequence of this

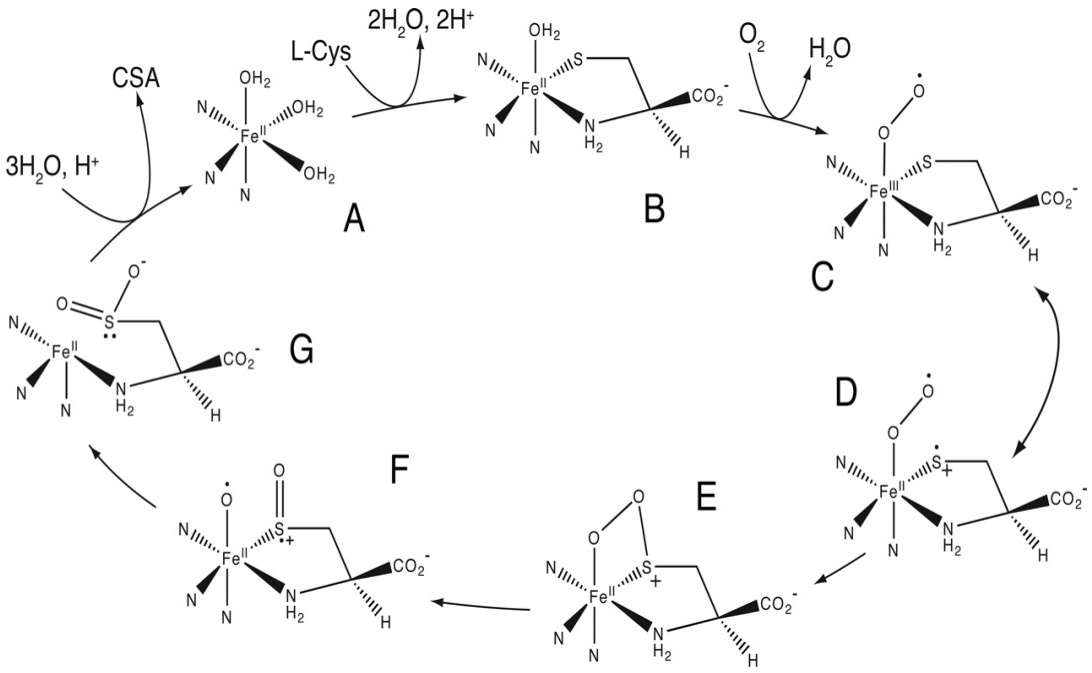

Figure 1.5. Proposed mechanism for CDO reaction (23).

ternary complex formation, the bound sulfur acquires partial cation-radical character (Figure 1.5 D), which can be stabilized by the adjacent negative charge on Tyr-157. Combination of bound sulfur and Fe(III)-superoxo gives a cyclic peroxo intermediate (Figure 1.5 E). Cleavage of the O–O bond leads to the formation of a sulfoxy cation and metal-bound activated oxygen (Figure 1.5 F). Transfer of the metal-bound activated oxygen results in the formation of the product, cysteine sulfinic acid (CSA) (Figure 1.5 G).

Within the same month, another three-dimensional crystal structure of CDO from *Rattus norvegicus* was solved to 1.5 Å resolution, and an alternative mechanism was postulated for cysteine oxidation (24) (Chapter 3). In this mechanism, the iron center can stabilize the superoxide radical instead of simple nucleophilic addition (Figure 1.6 A). Once O_2 binds to the Fe(II) center, O_2 accepts an electron from the iron and an H-bond from Tyr157 (Figure 1.6A complex 2). A putative base which is likely to be Tyr58, deprotonates the thiol of the substrate and transfers an electron to Fe(III) (Figure 1.6A complex 3). Radical coupling and cleavage of the oxygen-oxygen bond results in the formation of complex 4 and 5 as shown in Figure 1.6A. Rotation about the carbon sulfur bond gives complex 6. The subsequent addition of the iron-bound oxygen to the sulfur will give complex 7 and product dissociation completes this reaction.

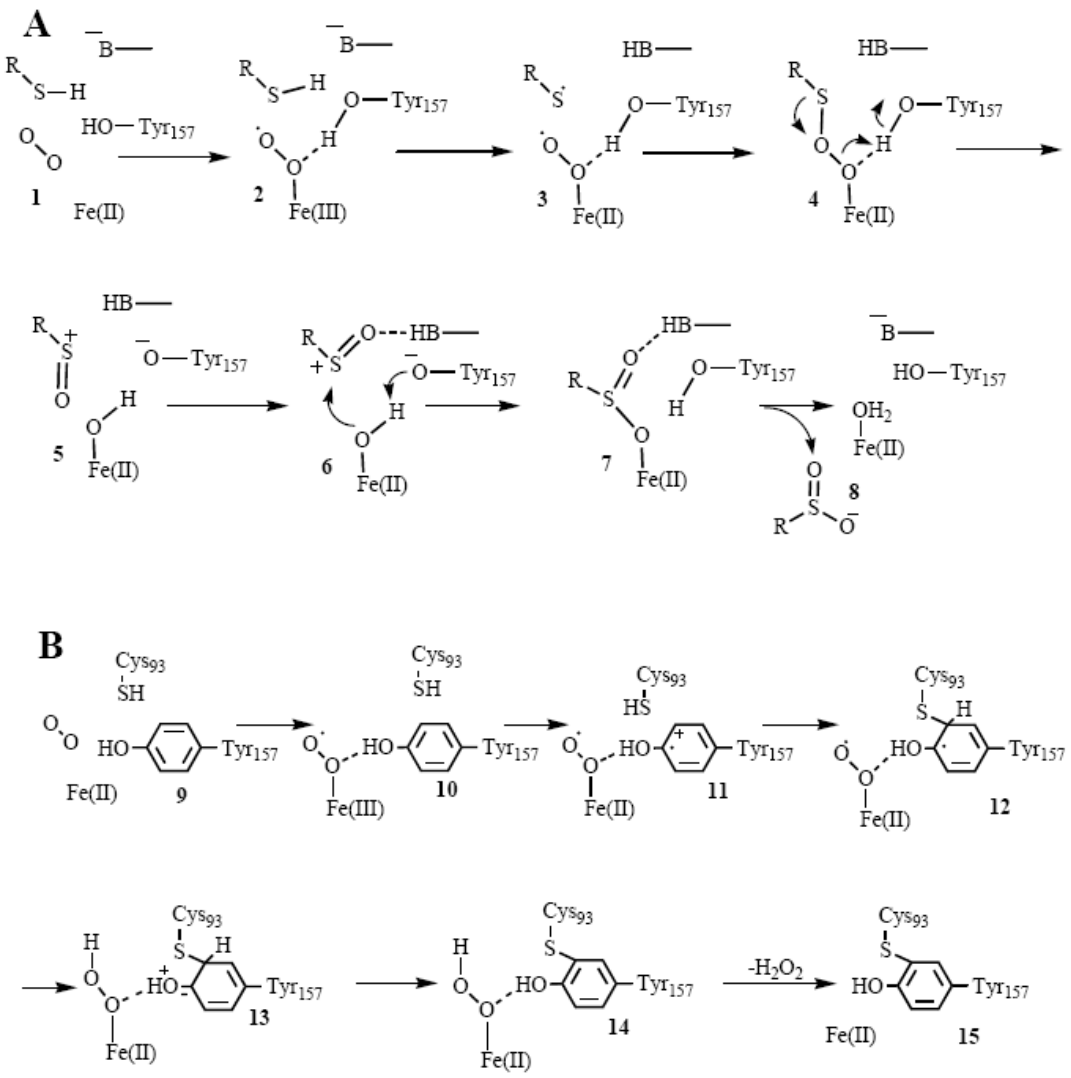

Figure 1.6. Mechanisms proposed for CDO. A). Mechanism for the catalytic cycle of cysteine oxidation. B). Mechanism for the formation of the cysteine-tyrosine linkage

In this mechanism, Tyr157 clearly participates in the catalytic cycle which offers a possible explanation of the activity loss of CDO after purification (Chapter 3). However, the above mechanisms have not been proven.

Little is known about the intermediates involved in the conversion of cysteine to CSA. Study of iron center binding by cysteine and its analogues only gives some information about the first step of the catalytic cycle. To identify reaction intermediates, studies of CDO with cysteine, oxygen, and its adducts are necessary. Because the electron paramagnetic resonance (EPR) signal of Fe^{2+} is silent and direct detection of O_2 adducts is difficult, the O_2 analogue, nitric oxide can be utilized to study the intermediates involved in O_2 activation. Nitric oxide has been a valuable probe for the study of many non-heme iron proteins because it has similar structural and electronic properties as O_2. The unpaired electron of NO makes a convenient spectroscopic probe because NO adducts formed by complexation with high spin Fe^{2+} are transformed into s=3/2 which exhibit EPR signals and Mössbauer spectra. Species produced by the reaction of Fe^{2+} with nitric oxide typically are brightly colored, and are designated as $\{Fe(NO)\}^7$.

In this paper, CDO from rat liver was cloned and expressed in *E.coli*. EPR studies of CDO with and without substrate were used to identify the changes in the active site of the iron center. In-gel digestion was used to extract the two bands of CDO from SDS-PAGE to identify the composition of each band. MALDI mass spectrometry was used to obtain

accurate molecular weights of the two forms of CDO observed by SDS-PAGE.

CHAPTER TWO

LITERATURE REVIEW OF THE PROTEIN FROM THE ALKANESULFONATE MONOOXYGENASE, SsuE

2.1 Identification of ssuEADCB genes and enzymes

In *Escherichia coli*, sulfate starvation leads to the increased synthesis of several starvation-induced (SSI) proteins involved in obtaining sulfur from alternate sources (26). The genes and proteins involved in this sulfonate-sulfur utilization have been identified by two independent approaches: two-dimensional gel electrophoresis and transposon mutagenesis with λ*plac*Mu9 (45, 46). The identification of these proteins was based on the assumption that the expression of SSI proteins would be repressed by sulfate and cysteine. By comparing cells grown with and without sulfate or Cys, several SSI proteins were identified which included the sulfate-binding protein (Sbp), *O*-acetyl serine lyase (CysK), cysteine-binding protein FliY, alkyl-hydroperoxide reductase C22 (AhpC), TauA, and D (SSI1, SSI2, SSI3, SSI5, SSI7, and SSI8). In addition, the genes encoding the proteins Ssi4 and Ssi6 have been mapped to the chromosome of *E. coli* by hybridization

analysis (1, 27). Five open reading frames were present and the operon was designated *ssu*EADCB (*ssu* for sulfonate-sulfur utilization) (Figure 2.1). The function of these genes and the proteins they encode were identified through mutagenesis studies. The genes *ssu*A, B, and C encode the ABC-type transport system for the uptake of aliphatic sulfonates, while *ssu*D and E encode the SsuD and SsuE proteins required for direct desulfonation of alkanesulfonates. Expression of the *ssu* genes requires the LysR-type transcriptional regulatory proteins CysB and Cbl. The CysB protein is regarded as the master regulator for sulfur assimilation in *E. coli* while the Cbl protein functions as an accessory element specific for utilization of sulfur from organosulfur sources (1).

2.2 Characterization of the two-component alkanesulfonate monooxygenase from Escherichia coli

SsuE and SsuD form the alkanesulfonate monooxygenase system, which is responsible for the acquisition of sulfur in bacteria. SsuE is the NAD(P)H-dependent flavin reductase which provides reduced flavin to SsuD. Following reduced flavin transfer, SsuD catalyzes the conversion of alkanesulfonates to the corresponding aldehyde and sulfite (Figure 2.2).

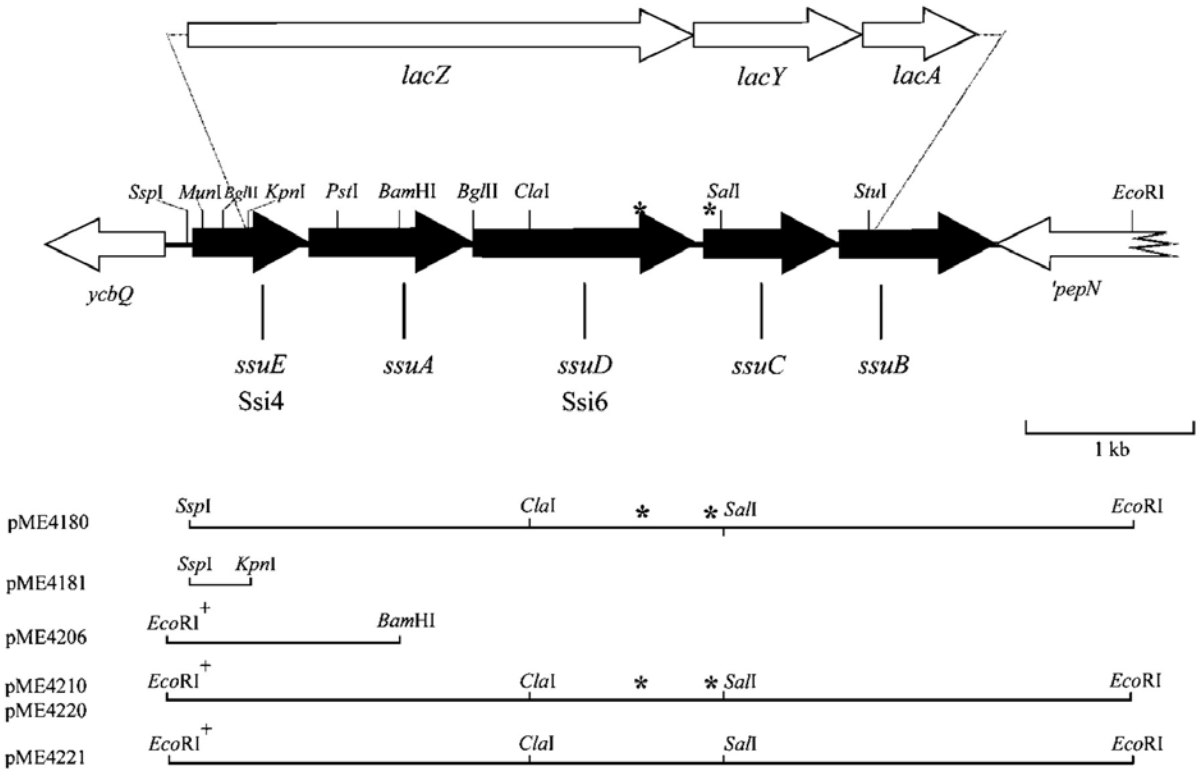

Figure 2.1. Organization of the *E. coli ssu*EADCB operon (27).

SsuE was first purified by expressing the cloned gene in *E. coli* strains DH5α and BL21(DE3). The purified SsuE lost activity in crude extracts, and the addition of a His tag to the wild type SsuE was eventually used to obtain pure and stable SsuE (5). An alternative purification protocol for SsuE lacking a His tag was developed in our laboratory (32) (Chapter 4.2.3). There was no significant loss of activity when SsuE was purified using ammonium sulfate fractionation, followed by hydrophobicity and anionic exchange chromatography. The addition of 100 mM NaCl and glycerol to the phosphate buffer helped stabilize SsuE.

Characterization of SsuE from *E. coli* has also been performed by our laboratory (32). The mass of SsuE is 21.3 Da determined by ESI mass spectrometric analysis. Sedimentation equilibrium analyses using multiple protein concentrations showed that SsuE exists as a dimer in solution. SsuE protein does not show a typical flavin absorption spectrum, indicating flavin is not a prosthetic group for SsuE. SsuE has been shown to reduce both FMN and FAD, while FMN is proposed to be the preferred substrate based on K_m values (5). Previous studies show that SsuE has a higher catalytic efficiency with NADPH compared to NADH, indicating NADPH is the preferred pyrimidine nucleotide substrate. Conversely, the results from our groups indicate that there is no significant difference in the catalytic efficiency of SsuE with either NADPH or NADH (30-32).

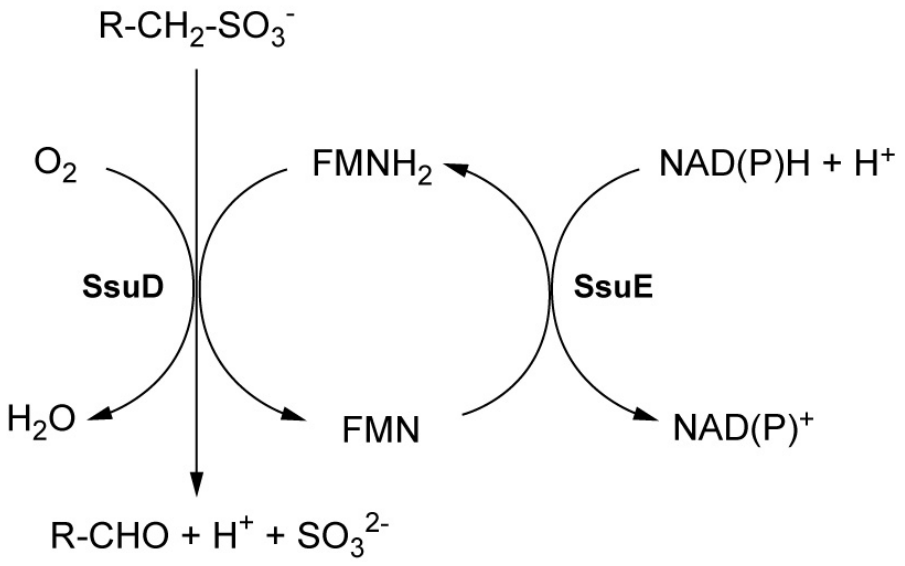

Figure 2.2. Proposed mechanism of the reaction catalyzed by the *E. coli* SsuD/SsuE alkanesulfonate monooxygenase system (25).

SsuD has been purified using a similar protocol with SsuE (5, 32). SsuD is a $FMNH_2$-dependent monooxygenase with a molecular weight of 41.6 kDa as determined by mass spectrometric analysis. SsuD is able to desulfonate C-2 to C-10 unsubstituted alkanesulfonates, substituted ethanesulfonic acids, N-phenyltaurine, and 4-phenyl-1-butanesulfonic acid. However, the preferred substrates for SsuD appear to be decanesulfonic acid, octanesulfonic acid, and 1, 3-dioxo-2-isoindolineethanesulfonic acid. Sedimentation equilibrium analyses have shown that SsuD is a homotetramer, and the ratio of SsuE:SsuD needed to achieve maximum activity is 2:1 (5, 32).

2.3 Kinetic studies of SsuE

The reduction of FMN by NADPH catalyzed by SsuE protein is a bisubstrate reaction (Figure 2.2). The mechanisms of such reactions normally fall into two major mechanistic classifications: sequential reactions in which all substrates must combine with the enzyme before any chemistry occurs, or Ping-Pong reactions in which one or more products are released before all substrates have been added. Sequential reactions can be further subclassified into ordered or random mechanisms. For the ordered mechanism there is a fixed order of substrate binding to the enzyme while the random mechanism has no preference for the order of substrate binding.

Plots of the initial velocity versus FMN concentration have been obtained by varying FMN concentrations at several fixed concentrations of NADPH (32). In addition, plots of the initial velocity versus NADPH were obtained by varying NADPH concentrations at several fixed concentrations of FMN. Both plots were best fitted to the equation for a sequential mechanism. However, they did not distinguish between an ordered or random mechanism.

Inhibition studies on SsuE were performed with $NADP^+$ as the product inhibitor to differentiate between an ordered or random mechanism (32). When the concentration of FMN was fixed at nonsaturating levels and the concentration of NADPH was varied at different concentrations of $NADP^+$, inhibition was observed with a K_i value of 13.6 ± 6 μM. Meanwhile, there was no apparent inhibition observed with saturating levels of NADPH, varied FMN concentrations, and different concentrations of $NADP^+$ indicating that the high NADPH concentrations were able to reverse the inhibition. The $NADP^+$ inhibitor showed a competitive inhibition pattern (Figure 2.3) which meant the NADPH substrate, and the $NADP^+$ product were competing for the free enzyme. This suggests that FMN reduction catalyzed by SsuE follows an ordered sequential mechanism (Scheme 2.1) (32).

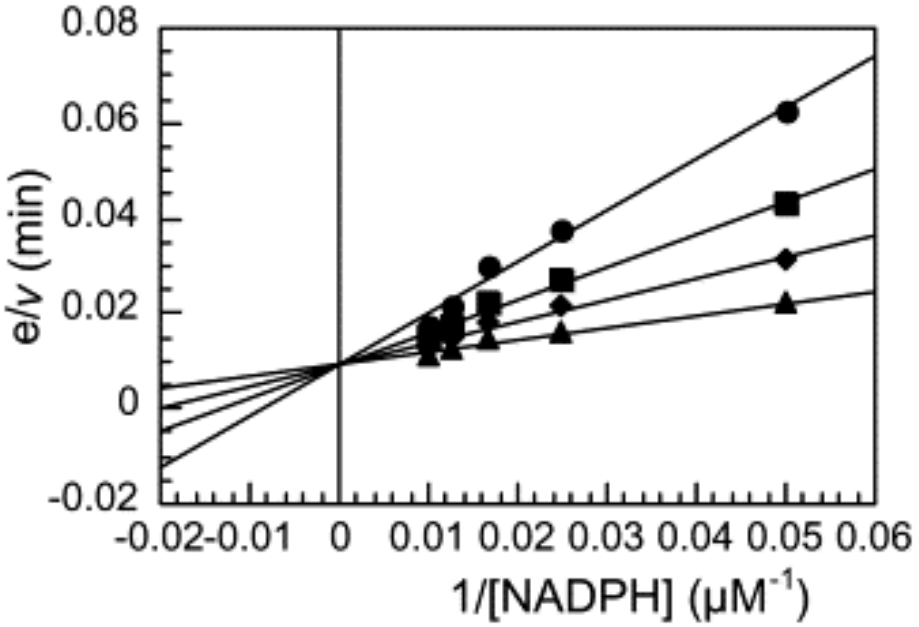

Figure 2.3. Inhibition of the SsuE enzyme by $NADP^+$. Assays were performed with 0.01 μM SsuE, 0.1 μM FMN, 20-100 μM NADPH, and varying [$NADP^+$]: 0 μM- triangles, 10 μM- diamonds, 20 μM- squares, 30 μM- circles (32).

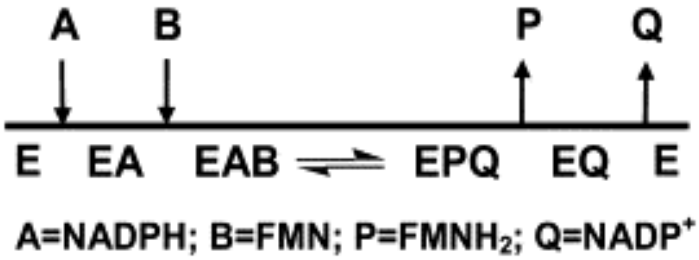

Scheme 2.1

Further experiments have shown that with SsuD and alkanesulfonate present, the mechanism of SsuE is modified from an ordered to a rapid-equilibrium ordered kinetic mechanism, and the K_d value of FMN is increased 10-fold. The change to a rapid equilibrium ordered kinetic mechanism displaces the reaction towards the ternary complex and subsequent flavin transfer. The lower affinity for FMN favors reduced flavin transfer from SsuE to SsuD. Therefore, flavin reduction by SsuE would lead to desulfonation of the alkanesulfonate substrate by SsuD instead of nonproductive oxidation.

2.4 Conserved residues in SsuE

The NAD(P)H:flavin reductase, Fre, from *E. coli* is a monomer with a molecular weight of 26.1 kDa, which reduces free FMN by NADPH or NADH. SsuE shares a similar catalytic function with Fre which belongs to the FNR family. At the amino acid sequence level, there is no significant homology between SsuE and other flavin reductases. However, previous studies reveal a conserved amino acid sequence, RXXS, in the FNR family which is important for recognition of the flavin isoalloxazine ring and catalysis. An alignment search of SsuE with the FNR family has shown that the conserved amino acid motif, $R_{51}XXS_{54}$, was also observed in SsuE (34, 35). (Figure 2.5)

```
              51   54

SsuE          R F D S

Fre E. c.     R P F S

Fre P. l      R P F S

Fre V. f      R P F S

FNR           R L Y S

PDR           R T Y S
```

Figure 2.4. Alignment of the RXXS motif of SsuE with the FNR family.

While there is no crystal structure for SsuE currently available, studies of the three-dimensional crystal structure of Fre protein with flavin bound do provide insight into the role of the specific active site residues in catalysis and flavin binding (36). In Fre protein, Ser49, Ser115 and Tyr116 form the inside of the isoalloxazine pocket. Tyr35, Phe48, Pro47, Asp227 and the main chain of residues 63-64 and 227-228 form the two walls of the pocket. Ser49 is positioned to form a hydrogen bond to N5 of the isoalloxazine ring. Consistent with this observation, Ser to Ala variant of Fre shows a 500-fold decrease in catalytic efficiency with a decreased affinity for oxidized flavin (36). The flavin binding site is hydrophobic due to a number of aromatic residues which provide hydrophobic and stacking interactions. The aromatic residue, Phe48, contacts with the *si* side of the isoalloxazine ring, which is also observed in other flavin reductase enzymes. At the polar edge of the isoalloxazine ring, N3 has been shown to bind to the carbonyl group of the protein. This has been confirmed by a decrease in the catalytic efficiency upon methylation of the N3 position. Fre has an Asp227 residue near the edge of the methyl groups of the isoalloxazine ring. This Asp residue may form a hydrogen bond to the catalytically important serine residue. In FNR, replacement of this residue with alanine causes a significant decrease in the electron-transfer rate between FNR and its substrates (37). Thus, this residue is supposed to participate in proton-coupled electron transfer during catalysis (35, 36).

Overall, the conserved motif, RXXS, has been observed in both the SsuE and the

FNR families. Because this motif plays an important catalytic role in the FNR family, the highly conserved amino acids, Phe52 and Ser54 identified in all SsuE proteins may play similar catalytic roles. Thus, in this thesis Ser54 and Phe52 of SsuE were substituted to Ala by site-directed mutagenesis and characterized through steady-state kinetic analysis. As a complementary method to mutagenesis studies, the pH profile of SsuE was determined.

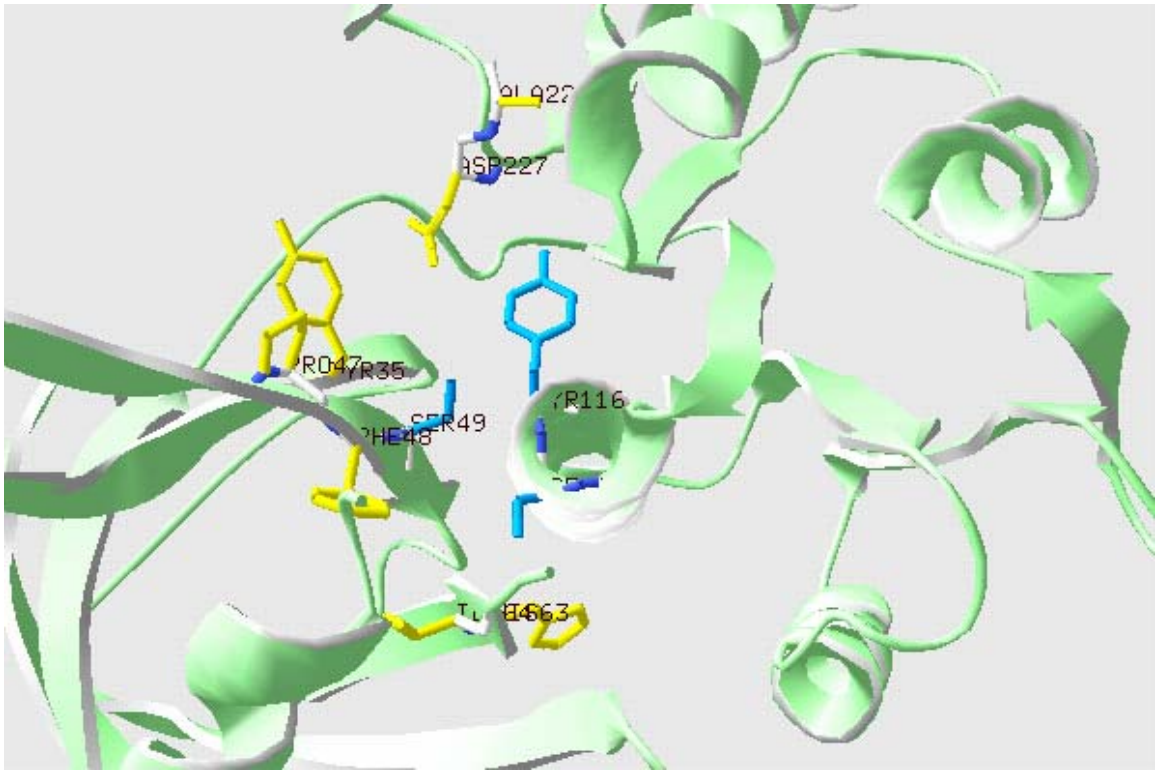

Figure 2.5. Isoalloxazine binding site of flavin reductase.

CHAPTER THREE

CHARACTERIZATION OF THE IRON CENTER IN CYSTEINE DIOXYGENASE

3.1 Statement of research objective for cysteine dioxygenase

The characterization of rat liver cysteine dioxygenase (CDO) expressed and purified from *E. coli* has been performed by few research groups (3, 12). A histidine$_6$ tag either N- or C-terminal has typically been linked to the CDO protein. As mentioned, the iron in CDO is coordinated by His86, His88, and His140 in a configuration similar to the 2-His-1-carboxylate triad of extradiol dioxygenase enzymes. It is reasonable to suppose that the histidine tag may sequester the iron targeted for the active site. Therefore, characterization of the iron center of CDO expressed without a His tag is necessary to fully and confidently determine the catalytic mechanism of CDO.

Purified recombinant CDO protein resolves as two bands by SDS-PAGE. The protein corresponding to the upper molecular weight band (~25.0 kDa) has higher catalytic activity than that of the lower molecular weight band (~23.0 kDa) (15). Previous

studies suggest a posttranslational modification may be responsible for the generation of the lower apparent molecular weight band. A focus of this research is to characterize the modification and determine how it affects the activity of CDO.

In this work, rat CDO without a His tag was expressed in *E. coli* and subsequently purified. Two bands were typically observed on SDS-PAGE following purification. SDS-PAGE, MALDI mass spectrometry, and HPLC were used to determine the composition of the two bands. In addition, atomic absorption and EPR were performed to investigate the role of the iron in the active site of CDO.

3.2 Materials and methods

3.2.1 Biochemical and chemical reagents

Matrices and protein standards used in MALDI were from Bruker. Potassium phosphate (monobasic anhydrous and dibasic anhydrous), sodium dithionite, sodium chloride, ampicillin, streptomycin sulfate, and lysozyme were from Sigma (St. Louis, MO). Isopropyl-β-D-thiogalactoside (IPTG), glycerol, tricholoracetic acid, and ammonium sulfate were purchased from Fisher Biotech (Pittsburgh, PA). Standard buffer contains 25 mM phosphate buffer, pH 7.5, and 10% glycerol. LB-Amp is LB medium

with 0.1 g/mL ampicillin added.

3.2.2 Construction of expression vectors

The individual cloning of the rat CDO genes into an expression vector was performed utilizing the Seamless Cloning System. The T7 RNA polymerase-dependent expression vector pET21a (Novagen, Madison, WI) was amplified using the primers 5' CAG TCA CTC TTC CCA TAT GTA TAT CTC CTT CTT, and 5' GCT TGC CTC TTC ACT CGA GCA CCA CCA CCA CCA including the *Eam*1104I restriction sites to produce *Nde*I and *Xho*I overhangs following digestion with the enzyme. The CDO gene was I.M.A.G.E. consortium clone ID 1769287. Primers 5' CAG TTT CTC TTC CGA GTT AGT TGT TCT CCA GTG AAC C, and 5' ATG GAA CGG ACC GAG CTG CTG were used to amplify the CDO genes which includes the *Eam*1104I restriction sites and engineered to produce *Nde*I and X*ho*I overhangs for ligation into the pET21A expression vector. DNA vectors containing representative clones were submitted for sequence analysis at Davis Sequencing (University of California, Davis).

3.2.3 Expression and purification of cysteine dioxygenase

BL21 (DE3) cells (*E. coli*) from a -80 °C stock containing the pET21a CDO vector were isolated on an LB-agar plate containing 100 μg/mL ampicillin (LB-Amp). A single

colony was used to inoculate 5 mL LB-Amp media, and the culture was incubated for 6 hours at 37 °C with shaking. A 1% inoculum of the 5 ml culture was used to inoculate 100 mL of LB-Amp media and the culture was incubated overnight at 37 °C. A 10 mL sample of the 100 mL culture was used to inoculate three flasks containing 1 L LB-Amp media. When the A_{600} value of the cells reached 0.5-0.6, the temperature was adjusted from 37 °C to 25 °C and isopropyl-ß-D-thiogalactocide (IPTG) was added to induce protein expression (the final concentration of IPTG was 0.4 mM). The cells were harvested after a 6 h incubation and centrifuged for 15 min at 5000g. The collected cells were then stored at -80 °C.

Cells from the 3 L growth were resuspended in 150 mL standard buffer containing 4 µg/ml of lysozyme. The cell suspension was sonicated and 1.5% (w/v) streptomycin sulfate was added to precipitate nucleic acids. The supernatant containing CDO was loaded onto a Macro-prep high Q column (Q column) and washed with 200 mL standard buffer. After the standard buffer wash, the protein was eluted by a linear gradient from 0-200 mM NaCl in standard buffer. The fractions determined to be pure by SDS-PAGE were pooled and $(NH_4)_2SO_4$ was added to a final concentration of 20% (w/v). The sample was then loaded onto a phenyl Sepharose column followed by a 200 mL wash with 20% $(NH_4)_2SO_4$ solution and eluted by a linear gradient from 20%-0% $(NH_4)_2SO_4$ in standard buffer. A final wash with 150 mL standard buffer was used to elute the CDO protein and the fractions were collected. The fractions were analyzed by SDS-PAGE and the

appropriate fractions which contained pure CDO protein were pooled. Because there was little Fe supplied in the culture medium, $Fe(NH_4)_2(SO_4)_2$ was added to the purified protein (Fe/CDO=1.2:1). The CDO protein was then dialyzed against 1 L standard buffer containing 100 mL NaCl and stored at -80 °C until further use.

3.2.4 Determination of the Fe/CDO ratio

Two methods were used to determine the iron content in CDO: UV-vis and atomic absorption spectroscopy.

For UV-vis spectroscopy, tricholoracetic acid (TCA) was added to precipitate the protein so the Fe ions were released from the protein. Ferene (0.2 mM) was added to form a complex with Fe^{2+} and Fe^{3+} ions which can be detected at 562 nm. The standard curve of iron was determined by plotting absorbance at 562 nm against different concentrations of $Fe(NH_4)_2(SO_4)_2 \cdot 6H_2O$ (0-30 nmols). The equation Y=A+BX was used to determine the best fit curve, where X represent the iron concentration in nmols, Y is the absorbance of the ferene complex from different concentrations of iron at 562 nm. The best fit curve was achieved using Kaleidagraph.

For atomic absorption spectroscopy, the lengths of different phases were as follows: drying phase, 85 °C for 5 secconds, 95 °C for 40 seconds and 120 °C for 10 seconds;

ashing phase, 700 °C for 8 secs; atomic excitation phase, 2300 °C for 5.1 seconds total. The concentrations of Fe used to establish the standard curve were 2.5, 5.0, and 10.0 µg/L. The concentration of CDO used was 0.089 µM (5 µg/L).

3.2.5 CDO activity

The activity of CDO was determined by monitoring oxygen consumption using a Clark-type O_2-sensitive electrode. After calibrating the electrode against the standard buffer, standard buffer containing 100 mM NaCl, 10 µM L-cysteine, and 10 µM dithionite were added to the chamber first and background oxygen consumption was monitored. CDO (5 µM) protein was then added and the rate of oxygen consumption was determined by calculating the slope of oxygen consumption versus time.

3.2.6 Electron paramagnetic resonance spectroscopy

EPR spectra of CDO (Fe^{3+}) with, and without L-cysteine, were recorded on a Bruker EMX spectrometer. The settings were as follows: Power, 99.85 µW; Frequency, 9.381 GHz; Mod amplitude, 10.00 G; and temperature, 10K. Cooling of the sample was performed with an Oxford Instruments ESR 900 flow cryostat with an ITC4 temperature

controller.

3.2.7 In- gel digestion and matrix assisted laser desorption ionization time of flight mass spectroscopy (MALDI-TOF)

The two bands of CDO at ~25.0 kDa and ~23.0 kDa were separated by 15% SDS-PAGE and excised from the gel. A 100 µL solution of 25 mM NH_4HCO_3/50% acetonitrile was added to the gel slices and vortexed for 10 min to remove the coomasie stain. The supernatant was extracted from the gel slices and the gel slice was washed two additional times and placed in a Speed Vac. After drying the gel slices, 500 µL of 25 mM NH_4CO_3 and 50 µL 10% SDS were added to both tubes and incubated overnight at 37 $^{\circ}$C to extract the protein. The supernatant was then transferred to a microfuge tube for further washing to remove SDS and glycerol. Water or 25 mM bicarbonate was used as the washing solution. The protein extracted from the gel was analyzed by MALDI-TOF mass spectrometry.

For MALDI-TOF mass spectroscopy, three matrix solutions were tested and sinapic acid (SA) yielded the best results. A buffer (200 µL) containing acetonitrile to 0.1%TFA in a 1: 2 volume ratio was used to dissolve 25 mg SA matrix. A 1 µL SA solution was mixed with 1 µL of the CDO protein sample (50 µM) and 1 µL of the mixture was

transferred to the plate for mass spectrometric analysis. The settings for the MALDI-TOF mass spectrometry (Microflex, Bruker, Billerica, MA) were as follows:

Acquisition operation mode, linear; Laser repetition rate in Hz, 10 psec; Reflector detector voltage, 0; Ion source voltage 1, 20; Ion source voltage 2, 18; Ion source lens voltage, 6.5; Number of shots, 40. The laser power used was between 45%-65% the maximum power.

3.3 Results

3.3.1 Purification of CDO

The results from different steps of the purification of CDO are shown in Figure 3.1. Interestingly, only one band at ~25.0 kDa (the upper molecular weight band) was present in the cell pellet (Lane 2) and a lower molecular weight band at ~23.0 kDa was present in the cell supernatant and subsequent purification steps (lane 3, 4, 5). The intensity of the two bands appeared equivalent following purification of CDO. However, the activity of CDO decreased corresponding with the appearance of the lower molecular weight band.

3.3.2 Iron content of CDO protein

Because iron is essential for CDO activity, it is necessary to determine the quantity of

iron in the expressed CDO protein prior to activity assays and EPR studies. The best fit curve from the UV-vis spectroscopy method was: y= -0.0022 + 0.0275x, R=0.9997. The amount of the iron was determined as 2.45 nmol, compared to the protein concentration of 5 nmol. The stoichiometry of iron bound to CDO determined by UV-vis spectroscopy was 0.5:1. For atomic absorption spectroscopy studies, the iron content was measured at 562 nm and the best fit curve was established as: $A_{562} = -0.0038C^2 + 0.083C + 0.0063$, where C represents the concentration of Fe. The average A_{562} for the sample was 0.3885, corresponding to an iron concentration of 6.6 μg/L or 118 nM relative to the protein concentration 89 nM. The stoichiometry of iron bound to CDO was 1.3:1.

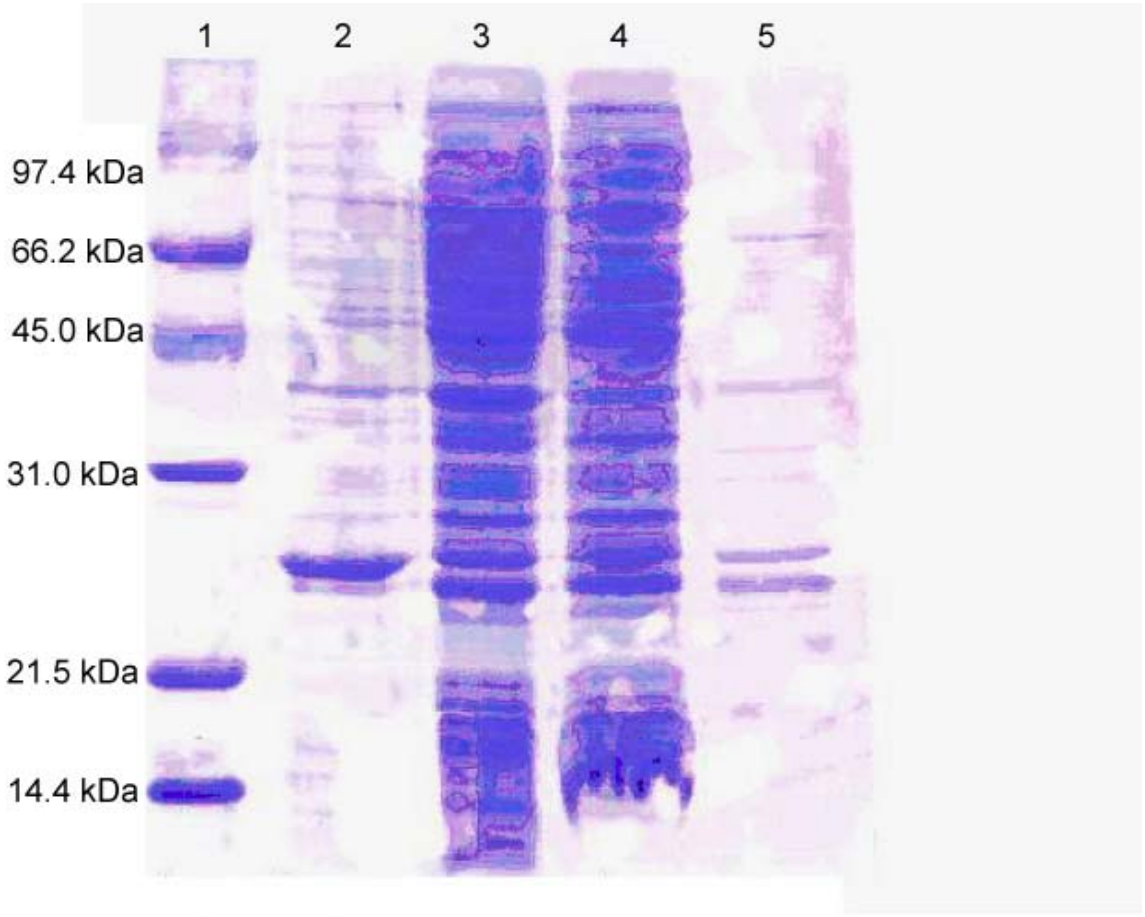

Figure 3.1. Purification of rat CDO. Samples from each step of the purification were separated on 12% SDS-PAGE. Lane 1- marker, Lane 2- cell pellet, Lane 3- supernatant after sonication, Lane 4- 1.5% streptomycin sulfate, Lane 5- fraction from Q-column.

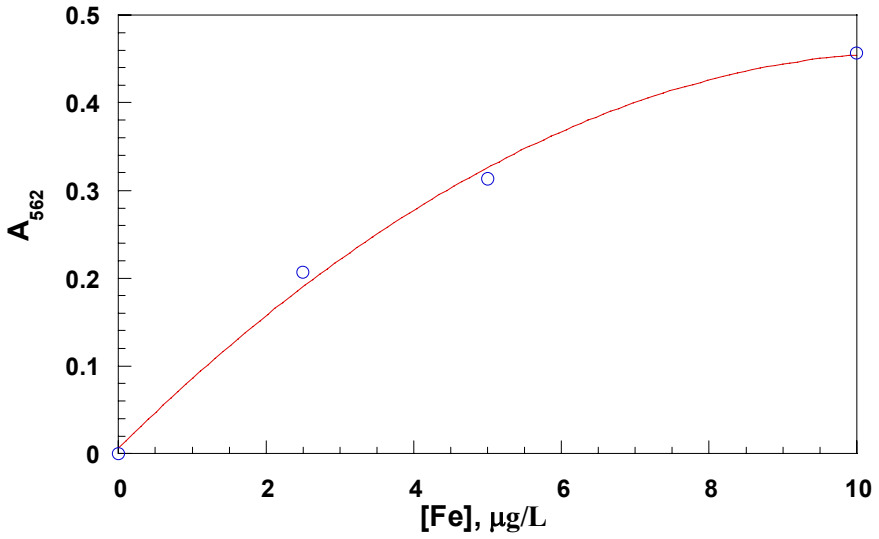

Figure 3.2 Iron standard curve from atomic absorption spectroscopy.

3.3.3 MADLI-TOF mass spectrometry of CDO

Purified CDO resolved as two bands by SDS-PAGE with apparent molecular weights of 23.0 (lower molecular weight band) and 25.0 kDa (upper molecular weight band). Results from protein analyses of the separated bands by LC/MS/MS showed no apparent difference in amino acid sequence. To obtain a more accurate molecular weight of CDO, the solution containing the 23.0 and 25.0 kDa forms of the protein were analyzed by MALDI-TOF mass spectrometry. Only one major peak with a molecular weight of 23.0 kDa was observed (Figure 3.3). This matches the calculated molecular weight of rat CDO from the amino acid sequence.

To optimize the signals obtained from MALDI-TOF mass spectrometry, the effects of buffers and sample concentrations were tested. Standard buffers and water were used to wash the CDO samples, and the standard buffer was shown to have a lower signal/noise ratio. The optimum concentration to obtain a distinct signal was 50 μM (Figure 3.4). CDO had only one apparent molecular weight from MALDI-TOF mass spectrometry while two bands were observed on SDS-PAGE. To further determine the difference between these two bands, they were separated by SDS-PAGE and extracted using the methods described in 3.2.7. Only single bands were observed when each of the separated bands were resubjected to SDS-PAGE (Lane 2 and 3 in Figure 3.5). Following tryptic digestion, the peptides were eluted by HPLC, and there was no clear difference between

the two bands (results not shown). The digested bands were also analyzed by MALDI-TOF mass spectrometry but no peaks could be identified.

3.3.4 EPR spectroscopy of CDO

EPR spectroscopy was performed to investigate the environment of the iron center. There was a clear difference in the EPR signals of the CDO Fe^{3+} center with and without L-cysteine (Figure 3.6). CDO with and without L-cysteine showed peaks at g=4.44 and g=4.36, respectively. Additionally, the peak appeared sharper with L-cysteine bound to CDO. These results suggest that cysteine directly affects the environment of the Fe center of CDO.

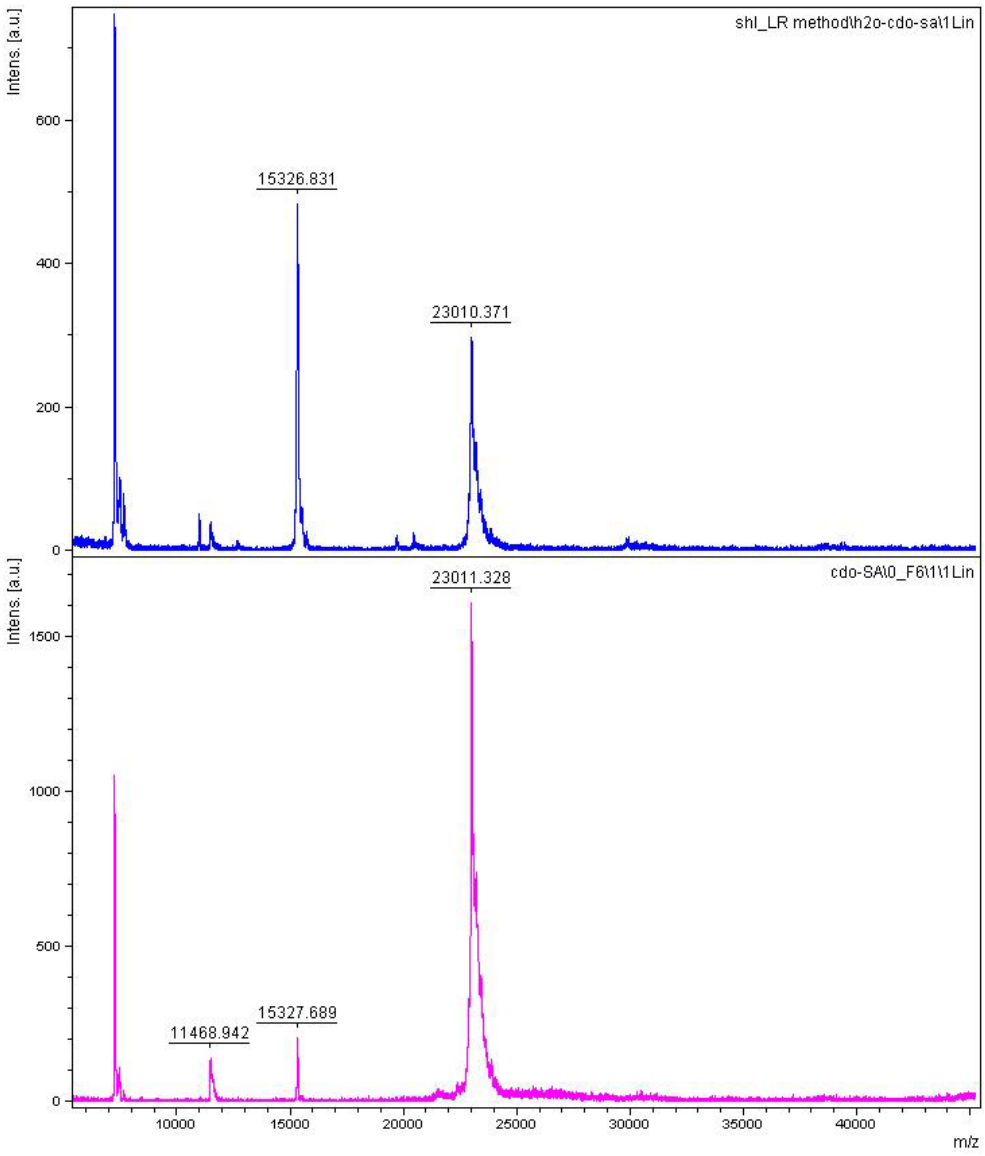

Figure 3.3. Buffer effects on the CDO signal from MALDI-TOF mass spectrometry. Upper panel- CDO washed with water; Lower panel- CDO washed with standard buffer (10% glycerol, 25 mM KPi, pH 7.5).

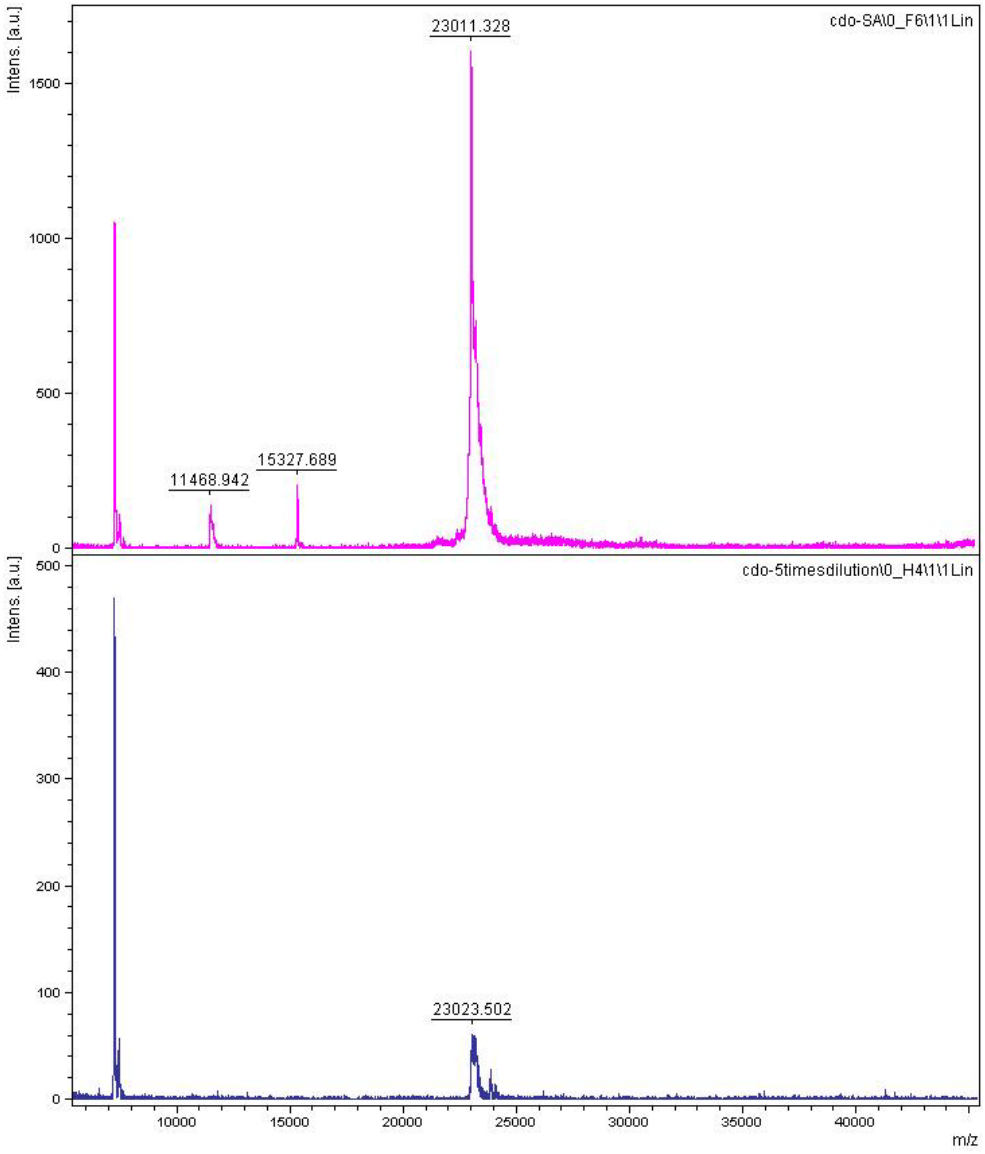

Figure 3.4. Dilution effect on the CDO signal from MALDI-TOF mass spectrometry. Upper panel- CDO protein (50 μM); lower panel- 5 times diluted CDO (10 μM).

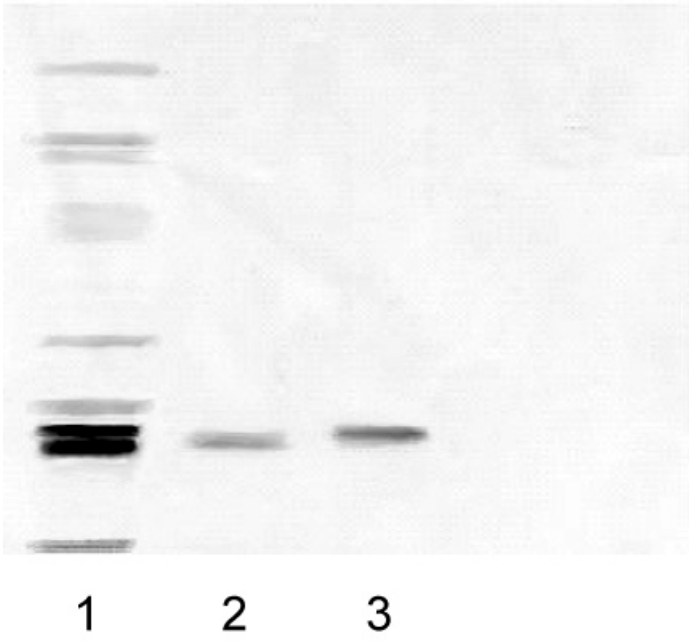

Figure 3.5. Separation of CDO on 12% SDS-PAGE gel. Lane 1- purified wild type CDO, lane 2- lower molecular weight band, lane 3- upper molecular weight band.

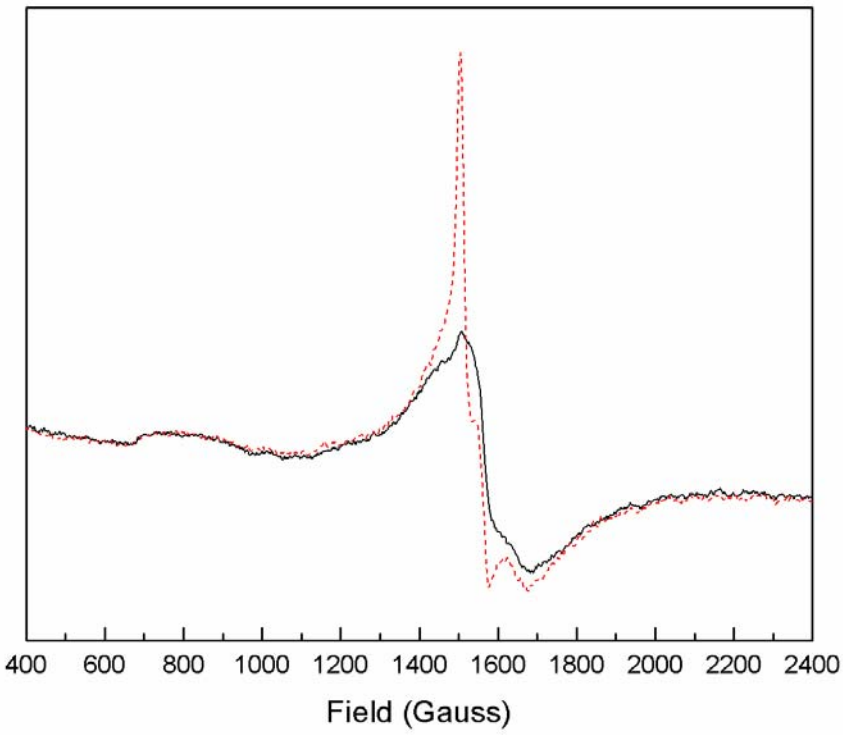

Figure 3.6. EPR spectrum of CDO (Fe^{3+}) with and without L-cysteine. Dotted line- CDO (Fe^{3+}) in 25 mM potassium phosphate buffer with pH 7.5, at 5 K; Solid line- CDO (Fe^{3+}) incubated with L-cysteine at 1:1.2 ratio in 25 mM potassium phosphate buffer with pH 7.5, at 5 K. The concentration of CDO and L-cysteine was 67.0 μM and 80.4 μM, respectively.

.

3.4 Discussion

3.4.1 Characterization of CDO

Because the CDO protein was expressed in *E. coli*, there was not a sufficient supply of iron provided in the LB media. Additional iron (iron/CDO=1.2:1) was added to the CDO protein following elution from the Phenyl Sepharose column. After dialysis to remove excess iron the Fe/CDO ratio was determined. From UV-vis spectroscopy the ratio of Fe/CDO was 0.5:1 while it was 1.3:1 from atomic absorption spectroscopy. One possible reason for the discrepancy in the UV-vis spectroscopy method is that the iron ions were not completely released when the protein was precipitated. Atomic absorption spectroscopy is more accurate because it detects all the iron in the sample solution. Overall the iron to CDO ratio is approximately 1:1 which was in good agreement with previous reports of 0.8:1 for protein purified from rat liver (8, 9). Most recombinant CDO including the CDO used in determining the three-dimensional structure contains a much lower iron content (10% iron content) following purification (23, 24). One reason for the discrepancy may be that no additional iron was added following purification. The addition of excess iron during the purification will allow for the complete formation of the iron center.

3.4.2 Isoforms of CDO

CDO has two bands on SDS-PAGE following purification. Interestingly, CDO protein from the cell pellet (Lane 2 in Figure 3.1) showed only one band (the upper molecular weight band, ~25.0 kDa) by SDS-PAGE. The lower molecular weight band was present in the cell supernatant and in following purification steps. Concomitantly, the intensity of the upper band decreased (Lane 3, 4, 5 in Figure 3.1). The two bands became equal in intensity after elution from the Q-column following purification (Figure 1, lane 5). Meanwhile, the activity of CDO decreased such that it was not even detectable ten hours after separation of the protein from the cell lysate. This activity loss correlated with the increase in intensity of the lower molecular weight band (23.0 kDa) and the decrease in intensity of the upper molecular weight band (25.0 kDa).

Elution fractions from the Q column were mixed with purified CDO, and there was still no observable activity. This excluded the possibility that the decrease in activity was caused by the removal of cellular components which were important in maintaining CDO activity. Anaerobic incubation of CDO with L-cysteine in the presence of reducing reagent did not recover the activity. Therefore, the activity loss appeared to be irreversible.

When the two bands extracted from SDS-PAGE were analyzed by MALDI-TOF mass spectrometry, no peaks were identified. The spectrum of diluted CDO showed that low

concentrations of CDO could be the main reason for the lack of identifiable peaks. The impurity of the sample due to residual components such as SDS, coomasie blue stain, and glycerol may also lead to an increased signal/noise ratio. After tryptic digestion, these two bands did not show the typical peaks for CDO on MALDI suggesting the traditional in-gel digestion protocol could not be utilized in these studies.

The apparent molecular weight of purified CDO from SDS-PAGE was ~23.0 and ~25.0 kDa. Previous mass spectrometry studies of recombinant CDO showed two molecular weights for CDO at 24.1 and 24.3 kDa, however the reason for these differences was not determined (15). Our results using MALDI-TOF mass spectrometry showed one major peak at 23.0 kDa which was similar to the calculated molecular weight of CDO (23.0 kDa). LC/MS/MS analysis of these two bands showed that they were identical in amino acid composition. The ~1 kDa difference of CDO molecular weight between previous results and our results maybe caused by the His tag.

More than one isoform of CDO was postulated according to the identification of multiple molecular weight forms of CDO (~23.0 kDa, ~25.0 kDa, and 68.0 kDa) (7, 15). From MALDI-TOF and amino acid sequencing results, it is clear CDO has only one form with a molecular weight of 23.0 kDa. The apparent molecular weights of 23.0 kDa and 25.0 kDa determined by SDS-PAGE both corresponded to the 23.0 kDa weight on MALDI while the 23.0 kDa one is the modified form of CDO. A possible reason that the

native CDO (23.0 kDa molecular weight from MALDI-TOF) showed a 25.0 kDa band on SDS-PAGE is that the accuracy of SDS-PAGE is lower than MALDI-TOF mass spectrometry.

Earlier studies suggested the conversion of the upper molecular weight band to the lower band was due to SDS-PAGE or buffer artifacts (15). Recently, the three dimensional crystal structure of rat CDO revealed a crosslink between Tyr157 and Cys93 near the active site (Figure 3.7) (23, 24). Based on recent studies, we have concluded that the crosslink was responsible for the two bands on SDS-PAGE, and oxygen initiated the formation of this crosslink. The CDO protein forms the crosslink due to oxidation only after it is extracted from the cells, and the crosslink in turn decreases the activity of CDO. Thus, the activity is decreased, and the apparent size of CDO is smaller on SDS-PAGE than the wild type protein. The crosslink did not and would not be expected to significantly alter the apparent mass of the protein when analyzed by mass spectrometry.

Identification of the cysteine-tyrosine crosslink in CDO suggested that this modification may lead to a loss in activity after purification (24). It has been shown that the mechanism for this type of modification is often related to the catalytic mechanism of the enzyme (Figure 3.8). As shown in Figure 3.8 B, it requires electron transfer from the active site Fe(II) to molecular oxygen followed by the formation of a superoxide complex. Electron transfer from Tyr157 to Fe(III), addition of the thiol to the benzene ring, and

aromatization followed by dissociation of hydrogen peroxide complete this modification (24). Thus, in the presence of oxygen and lack of Cys substrate, Tyr157 forms a covalent crosslink with Cys93 which will decrease or even eliminate the ability of Tyr157 to participate in the oxidation of the cysteine substrate.

From the results above, it can be concluded that the upper molecular weight band (~25.0 kDa) which does not possess a Tyr-Cys crosslink is the physiologically active form of CDO. Due to the loss of its reducing environment, wild type CDO is susceptible to oxidation and a crosslink inside the active site is formed during purification. Thus, the protein with the crosslink appears to have a lower molecular weight than the unmodified protein on SDS-PAGE. Meanwhile the activity of CDO decreases as the upper molecular band is oxidized until there is no detectable activity. The upper molecular weight band was not completely converted to the lower molecular weight band because the oxidation requires the reduced form of Fe which is limiting under aerobic conditions. The involvement of Tyr157 in the modification could be responsible for the activity decrease.

There are several possible methods to avoid formation of the crosslink. One is to purify CDO under anaerobic conditions and assay for activity. A second method is to substitute Cys93 with alanine because it does not appear to play an essential role in catalysis. Another possible way is to add an oxidant like ferri cyanide after breaking the cell. So the iron center of CDO will be oxidized and could not catalyze the formation of

the crosslink. Recent studies in our laboratory have shown that mutation of Cys93 or Tyr 157 to alanine resulted in the exclusive production of a protein migrating at ~25.0 kDa molecular weight. Therefore, the crosslink between Tyr157-Cyr93 is responsible for the presence of the two bands on SDS-PAGE. The role of Tyr157 in both the formation of the covalent crosslink and catalysis of cysteine oxidation is currently being investigated.

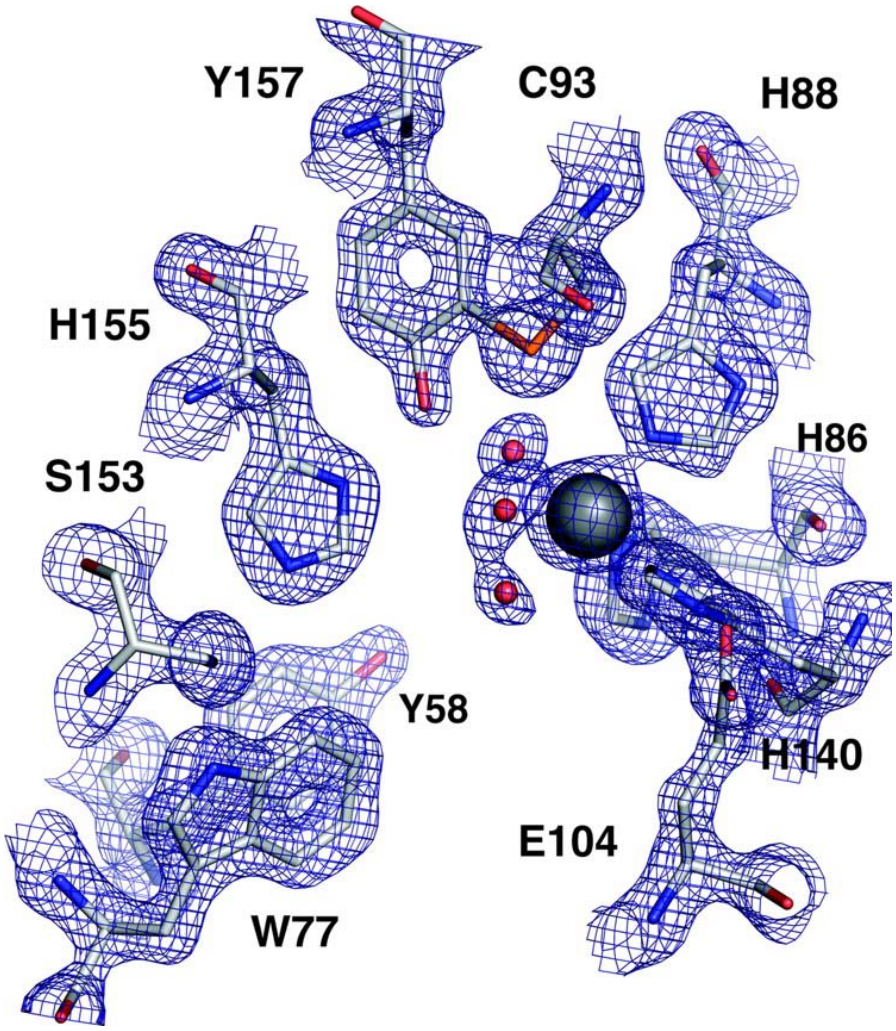

Figure 3.7. CDO active site contoured at 1.2σ. The metal is shown as the g solid black sphere; His-86, -88, and -140 are the metal ligands. Three additional coordination sites are occupied by water. Cys-93 and Tyr-157 are covalently linked, and the hydroxyl group of Tyr-157 is 4.4 Å from the metal. Other conserved active-site residues are highlighted (23).

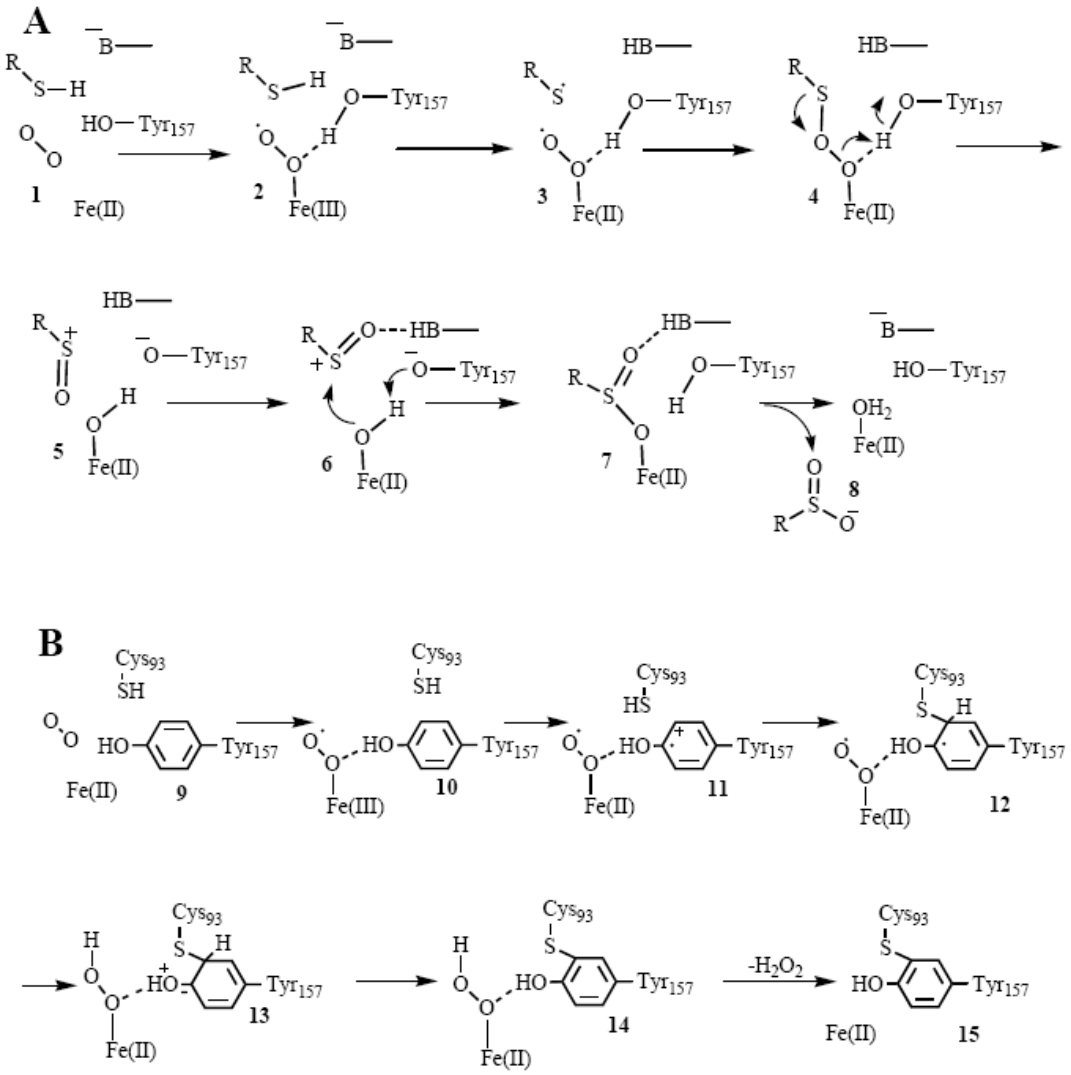

Figure 3.8. Proposed mechanisms for CDO. A. Mechanism for the catalytic cycle of cysteine oxidation. B. Mechanism for the formation of the cysteine-tyrosine linkage (24).

3.4.3 EPR spectroscopy studies of CDO

EPR spectroscopy was performed to obtain information on the metal environment of CDO. Since Fe^{2+} is EPR silent, the oxidized form of CDO (Fe^{3+}) was analyzed by EPR. The g values obtained from EPR spectroscopy for CDO with and without L-cysteine changed from 4.36 to 4.44. In addition, the intensity of the EPR signal with L-cysteine bound to CDO is more pronounced. These results suggest cysteine incubation with CDO altered the environment of the iron center. This can be explained from the mechanism of CDO catalysis proposed by McCoy and coworkers (23). In the proposed mechanism for cysteine oxidation (Figure 1.5), L-cysteine binds to the iron center in a chelating mode using its sulfur and nitrogen atoms and displaces two water molecules which is the initial step of the cysteine oxidation. The coordination of L-cysteine to the iron center is necessary because the binding of L-cysteine will place the sulfur of L-cysteine trans to His140. This orientation distinguishes this coordination from other ligands to the iron, and makes this region of the active site favorable for oxygen binding. While the ferric form of the iron was shown to be the resting state of the enzyme, Cys may still be able to coordinate to the ferric form of CDO.

CHAPTER FOUR

RESEARCH OF THE FLAVIN REDUCTASE FROM THE ALKANESULFONATE MONOOXYGENASE SYSTEM

4.1 Statement of research objective

In *E. coli*, SsuD and SsuE constitute a two-component alkanesulfonate monooxygenase system which is responsible for the desulfonation of alkanesulfonate substrates. SsuD is a monooxygenase enzyme that catalyzes the desulfonation reaction with reduced flavin provided by SsuE.

SsuE-catalyzed reduction of FMN follows an ordered-sequential mechanism with NADPH as the first substrate to bind and $NADP^+$ as the last product to dissociate (32). Previous studies suggest a ternary complex is formed with FMN, NADPH, and SsuE before further catalysis occurs. The reduced flavin is then transferred to SsuD where a peroxyflavin intermediate is proposed to oxidize the alkanesulfonate.

Flavin transfer from SsuE to SsuD likely occurs through a direct transfer mechanism since reduced flavin is oxidized rapidly in air. Oxidized flavin binds to SsuE with a K_d of

0.015 μM. When SsuD is present, the K_d value of FMN for SsuE is altered to 0.13 μM, suggesting the interaction of the two proteins increases the rate of flavin transfer from SsuE to SsuD (32).

The conserved amino acid sequence for the FNR family, $R_{51}FDS_{54}$, has been observed in SsuE and has previously been shown to play an important role in flavin binding and catalysis. Based on this motif, substitutions of Phe52 and Ser54 to Ala were performed on SsuE by site-directed mutagenesis. The recombinant proteins, S54A and F52A SsuE, have been expressed, purified and studied through kinetic analyses. As a complementary method to the mutagenesis studies, the pH dependence of SsuE has been determined.

4.2 Methods and materials

4.2.1 Biochemical and chemical reagents

FMN, NADPH, $NADP^+$, potassium phosphate (monobasic anhydrous and dibasic anhydrous), sodium chloride, ampicillin, streptomycin sulfate, and lysozyme were from Sigma (St. Louis, MO). Isopropyl-β-D-thiogalactoside (IPTG), glycerol, and ammonium sulfate were purchased from Fisher Biotech (Pittsburgh, PA). LB-Amp is LB medium with 0.1 g/mL ampicillin added. Standard buffer contains 25 mM potassium phosphate, pH 7.5 and 10% glycerol.

4.2.2 Construction of expression vectors for S54A, F52A and wild type SsuE

The individual cloning of the SsuE gene into an expression vector was performed as previously described (32). The SsuE gene containing the F52A or S54A substitution was constructed using the QuickChange® site-directed mutagenesis kit (Stratagene, La Jolla, CA). The native SsuE construct was PCR-amplified with primers, 5' CTT GAG TGC CGG CGC (where the mutation is) ATC GAA ACG AGC, and 5' GCT CGT TTC GAT GCG CCG GCA CTC AAG for S54A SsuE and 5' CTT TAT GCT CGT GCG GAT AGT CCG GC (forward primer), and 5' GCC GGA CTA TCC GCA CGA GCA TAA AG (reverse primer) for F52A SsuE. The PCR-amplified products were then analyzed on a 1% agarose gel. After cleanup and addition of 1 μL *Dpn* I restriction enzyme to remove the template plasmids, the PCR plasmid was transformed into XL1-blue supercompetent cells. For the transformation, 1 μL of each PCR product was added to 50 μL competent cells and the cells were incubated on ice for 1 hour. The sample was heat shocked for 45 seconds at 42 °C and placed on ice for 2 minutes. 1 mL LB media was added to the sample and incubated at 37 °C with shaking for 1 hour. The culture was then centrifuged and the collected cells were plated on LB-Amp and incubated at 37 °C overnight. Representative colonies were selected and inoculated in 5 ml LB-Amp media. After an overnight incubation at 37 °C, the plasmid was extracted using the QIAprep® Spin

Miniprep kit (Stratagene, La Jolla, CA) and submitted for sequencing analysis. After the substitution was confirmed the S54A SsuE or F52A SsuE plasmid was mixed with 50% glycerol and stored at -80 °C.

4.2.3 Expression and purification of S54A, F52A, and wild type SsuE

Cells from frozen stocks were isolated on LB-Amp. A single colony of *E. coli* BL21(DE3) containing the appropriate expression plasmid was used to inoculate 5 mL LB-Amp media which was incubated for 7 h at 37 °C. A 1% inoculum of the 5 mL culture was used to inoculate 100 mL LB-Amp media which was incubated overnight at 37 °C. A 10 mL aliquot of the 100 mL culture was then used to inoculate 2 flasks containing 1 L LB-Amp media. When the A_{600} value reached 0.8–0.9 for SsuE, the temperature of the culture was adjusted from 37 to 18 °C, and isopropyl-β-D-thiogalactoside (IPTG) was added to a final concentration of 0.4 mM. The incubation was continued for 6 h and cells were harvested by centrifugation at 5000*g* for 15 min and stored at −80 °C.

For the purification of S54A, F52A, and wild type SsuE, cells from the 2 L growth were resuspended in 100 mL standard buffer containing 4 μg/mL lysozyme. Cell lysis was performed by sonication, followed by the addition of 1.5% (w/v) streptomycin

sulfate with stirring at 4 °C for 1 hour to precipitate nucleic acids. Ammonium sulfate precipitation was performed from 20-45%. The pelleted proteins from the 45% ammonium sulfate precipitation were resuspended in 150 mL standard buffer with 20% ammonium sulfate and loaded onto the phenyl Sepharose column. After washing the column with 20% ammonium sulfate buffer, the protein was eluted with a linear gradient from 20% to 0% ammonium sulfate in standard buffer (300 mL total volume), followed by elution with standard buffer alone. Fractions containing large A_{280} values were pooled and loaded onto a macro-prep high Q column. After washing the column with standard buffer, the protein was eluted with a linear gradient from 0 to 300 mM NaCl in standard buffer. Fractions determined to be pure by SDS–PAGE were pooled, precipitated with 45% ammonium sulfate to concentrate the protein, and resuspended in standard buffer containing 100 mM NaCl. The resuspended protein pellet was pooled, dialyzed against standard buffer containing 100 mM NaCl, aliquoted, and stored at −80 °C.

4.2.4 Circular dichroism of SsuE

The circular dichroism spectra of S54A, F52A, and wild type SsuE, were obtained on a J-810 spectropolarimeter (JASCO, Tokyo, Japan). The settings used were as follows: Scanning range, from 300 nm to 180 nm; Pitch, 0.1 nm; Scanning mode, continuous; Scan speed, 50 nm/min; Response, 1s; Bandwidth, 1 nm; Accumulation, 4; Protein concentration, 0.1 mg/ml; Cuvette path length, 0.1 cm.

4.2.5 Determination of kinetic parameters for S54A, F52A, and wild type SsuE

Determination of the kinetic parameters for FMN was performed by monitoring the changes in NADPH absorbance at 340 nm with 120 μM NADPH, 50 nM S54A, F52A or wild type SsuE and variable concentrations of FMN from 0.02 μM to 0.6 μM. The buffer used was standard buffer in 100 mM NaCl. The NADPH and FMN solutions were added first to measure the background rate due to autooxidation and the background was subtracted from the net rate to determine the initial velocity. From the NADPH absorbance changes the initial reaction velocity was measured and plotted versus the FMN concentration.

Fluorescence spectroscopy experiments were performed on a Perkin Elmer LS 55 luminescence spectrometer (Palo Alto, CA) to determine the K_d values. The excitation wavelength was set at 280 nm and the emission wavelength was 344 nm. The slit widths were set at 5 nm. For the fluorimetric titration experiments, 1.0 ml of 0.5 μM F52A, S54A, and wild type SsuE were titrated with FMN varied from 0.04 μM to 1.7 μM. The buffer used was standard buffer in 100 mM NaCl. The fluorescence spectrum was recorded following a 2 min incubation after each addition of 1 μl FMN. The bound FMN was determined by the following equation (32, 40).

$$[\mathrm{FMN}]_{bound} = [\mathrm{SsuE}]\frac{(I_0 - I_c)}{(I_0 - I_f)} \qquad \textbf{(1)}$$

where [SsuE] represents the initial concentration of enzyme, I_0 is the initial fluorescence intensity of SsuE prior to the addition of FMN, I_c is the fluorescence intensity of SsuE following each addition of FMN, and I_f is the final fluorescence intensity. The concentration of FMN bound ($[FMN]_{bound}$, y) was plotted against the total FMN ($[FMN]_{total}$, x) to obtain the dissociation constant (K_d) according to equation **2** where n is the binding capacity of SsuE (32, 40).

$$y = \frac{(K_d + x + n) + \sqrt{(K_d + x + n)^2 - 4xn}}{2} \qquad \textbf{(2)}$$

4.2.6 pH profile of wild type SsuE

The pH range used to determine the pH profile of SsuE was from 4.0-9.0. Acetic acid buffer was used for pH 4.0-5.5; succinic acid buffer was used for pH 5.0-6.5; phosphate buffer was used for pH 6.0-8.0; Tris-base buffer was used for pH 7.5-9.0. The pH overlap between buffers was used to determine if there were any alterations in activity due to buffer effects. The *V/K* value which reflected the information of both substrate binding and catalysis was plotted against the pH value changes.

4.3 Results

4.3.1 Expression and purification of S54A and F52A SsuE

According to the protocol described in 4.2.2, the substitution of Ser or Phe to Ala was introduced to the *ssu*E/pET21a plasmid through PCR amplification. The amplified products were analyzed on a 1% DNA agarose gel (shown as S54A, Figure 4.1). Lane 2 is the PCR product from 5 ng of template and lane 3 is from 10 ng of template. Following PCR clean-up and *Dpn I* digestion of the parental plasmids, competent cells were transformed with 1 μL of the PCR product. The plasmid from representative colonies was extracted using the QIAprep® Spin Miniprep kit (Stratagene, LA Jolla, CA) and submitted for sequencing analysis (University of Califonia, Davis). Sequencing analysis confirmed both mutations were introduced into SsuE.

The S54A and F52A SsuE proteins were purified using the same protocol as wild type SsuE (4.2.3). The protein yield from a 2 L growth was 30 mg-50 mg which was similar to wild type protein. To determine if the gross secondary structure was altered by the amino acid substitution, each protein was analyzed by CD spectroscopy (Figure 4.1). The spectra obtained for S54A and F52A SsuE were similar with wild type SsuE, suggesting that no gross secondary structural changes occurred due to the amino acid substitutions.

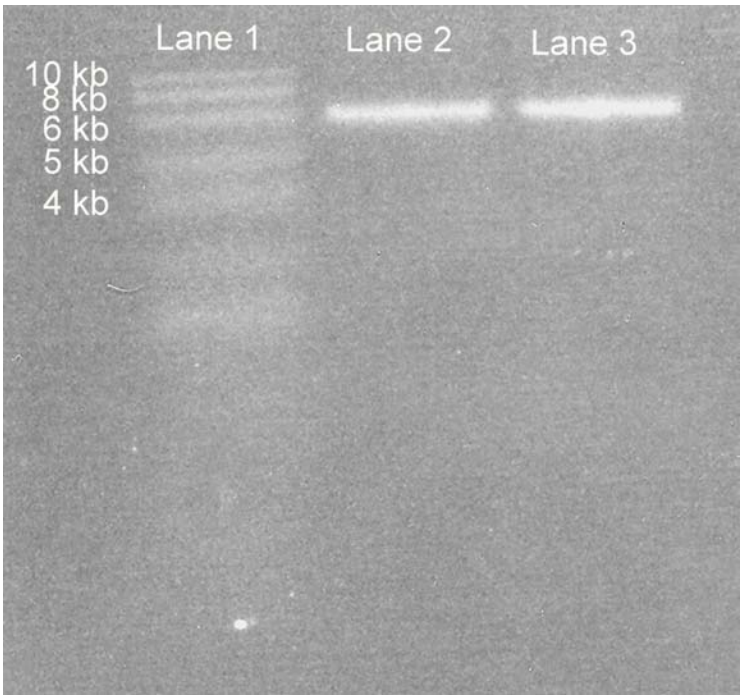

Figure 4.1. Agarose gel of PCR amplified S54A *ssu*E/pET21a plasmid. Lane 1- DNA marker, Lane 2- 5 ng s*su*E/pET21a plasmid was used as template, lane 3- 10 ng *ssu*E/ pET21a as template.

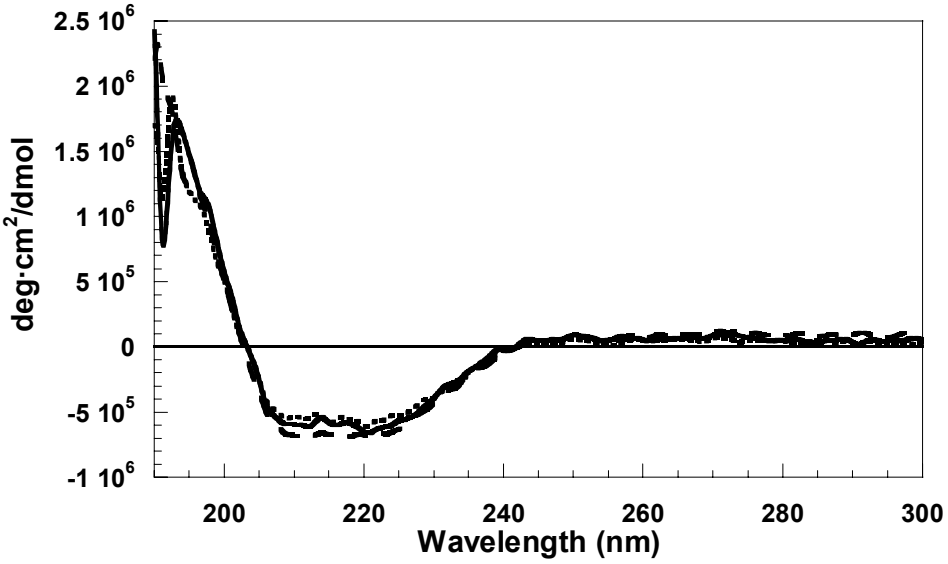

Figure 4.2. CD spectra of S54A, F52A and wild type SsuE. Solid line- wild type SsuE, dotted line- S54A SsuE, dashed line- F52A SsuE

4.3.2 Steady-state study of S54A and F52A SsuE

The initial reaction rates of FMN reduction by NADPH catalyzed by S54A and F52A SsuE were determined by monitoring the decrease in absorbance due to NADPH oxidation at 340 nm. The initial velocity versus FMN concentration was plotted and fitted to the Michaelis-Menton equation (Figure 4.3). The K_m values were 0.09 μM for S54A SsuE and 0.30 μM for F52A SsuE. Compared with wild type SsuE, the K_m values of S54A and F52A SsuE increased by 6 and 18-fold, respectively. The k_{cat} values of S54A and F52A SsuE were similar to wild type SsuE (Table 4.1).

Fluorometric titration experiments were performed to determine the K_d values for FMN binding (Figure 4.3, Figure 4.4A). The K_d value of S54A was 0.12 μM which was 8-fold higher than the value of wild type SsuE while the K_d of F52A was increased by 3-fold.

4.3.3 Determination of the pH profile of SsuE

The effect of pH on FMN reductase activity was investigated over a pH range from 4 to 9 using appropriate buffer systems. SsuE showed a broad optimal activity range between pH 4.5 and 9 where there was no significant change in the activity. In addition, there was no dramatic change in the activity of SsuE due to changes in the buffer system suggesting there were no buffer effects observed due to changes in buffer composition.

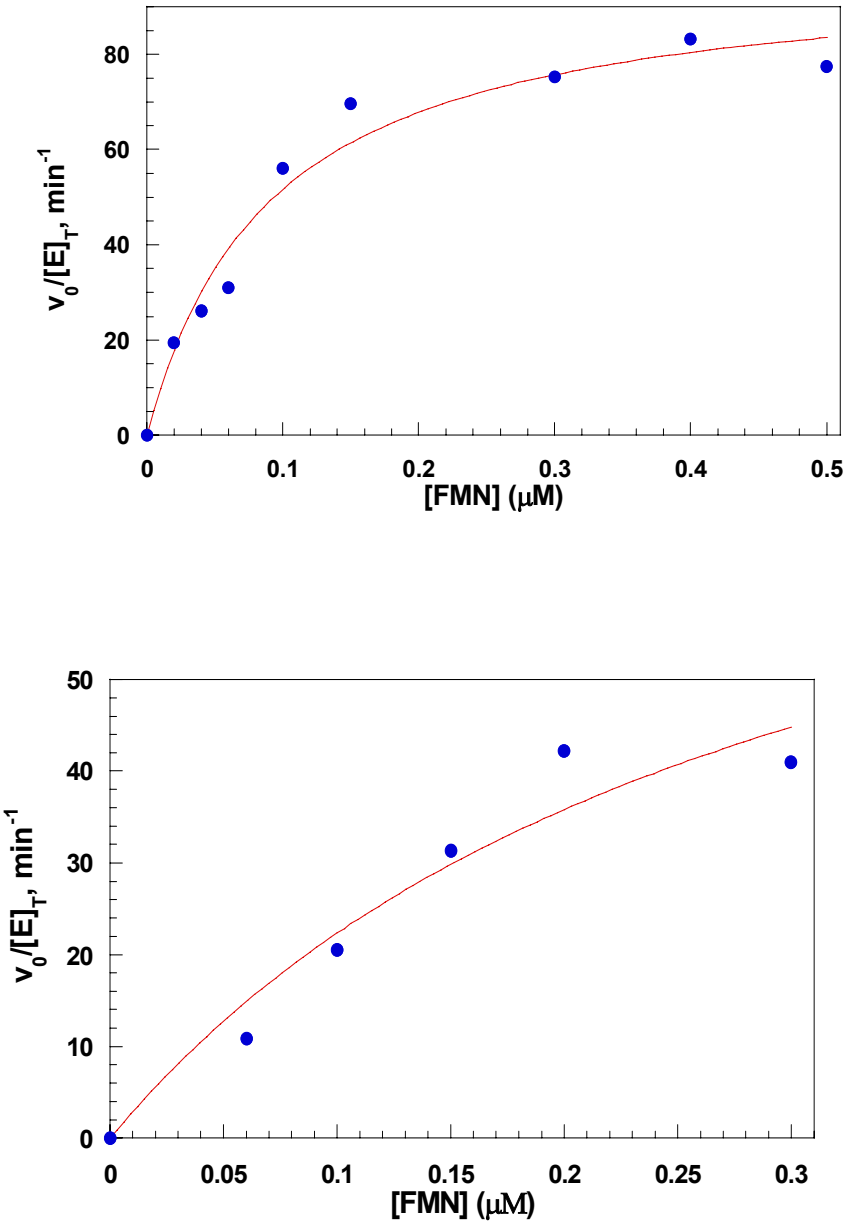

Figure 4.3. The initial reaction rate of FMN reduction catalyzed by S54A and F52A SsuE, $V_0/[E]_T$, plotted against the substrate concentration [FMN]. Upper plot- S54A SsuE, Lower plot- F52A SsuE.

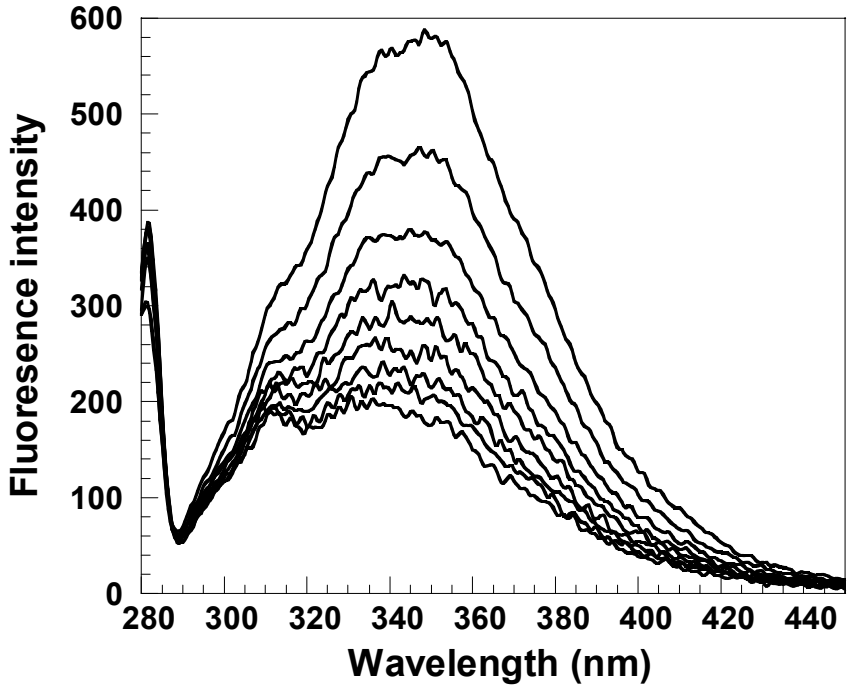

Figure 4.4. Fluorimetric titration of S54A SsuE by the addition of FMN.

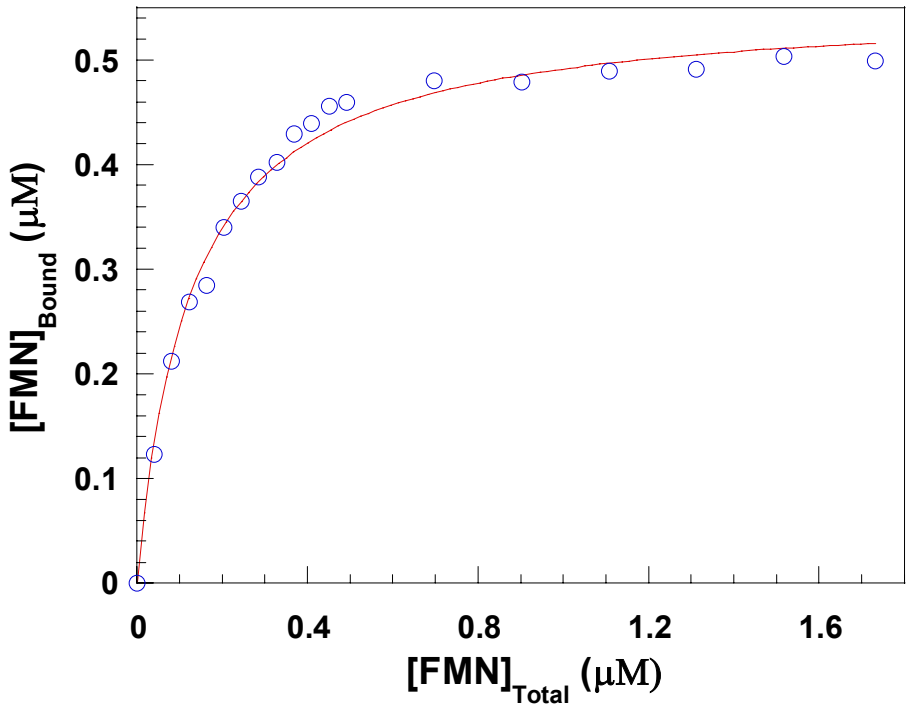

Figure 4.5. Determination of the K_d of S54A SsuE by plotting the bound [FMN] against the total [FMN]. S54A SsuE concentration was 0.5 μM, FMN concentration was from 0-1.8 μM.

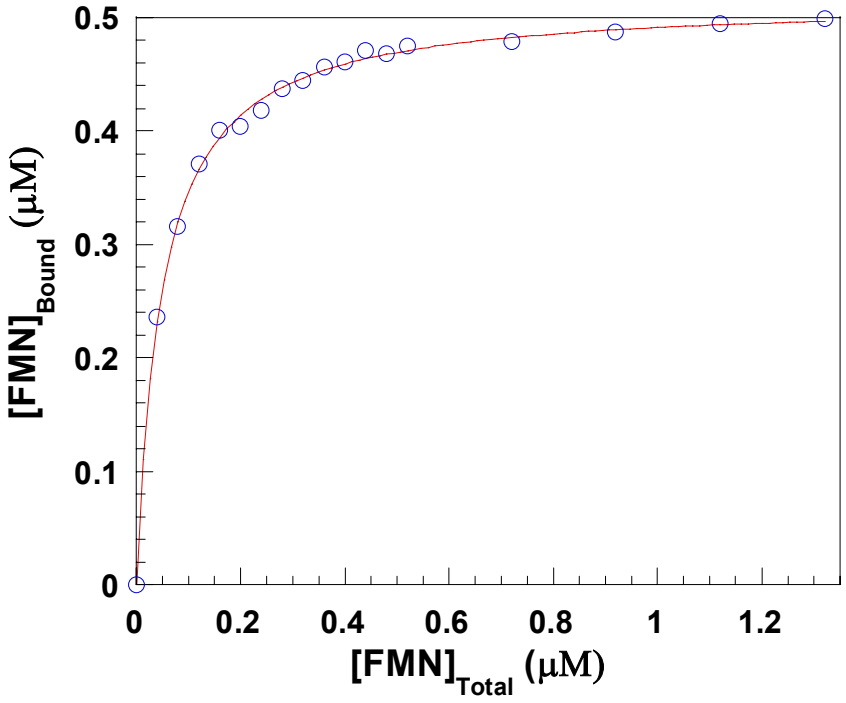

Figure 4.6. Determination of the K_d of F52A SsuE by plotting the bound [FMN] against the total [FMN]. The F52A SsuE concentration was 0.5 μM, FMN concentration was from 0-1.5 μM.

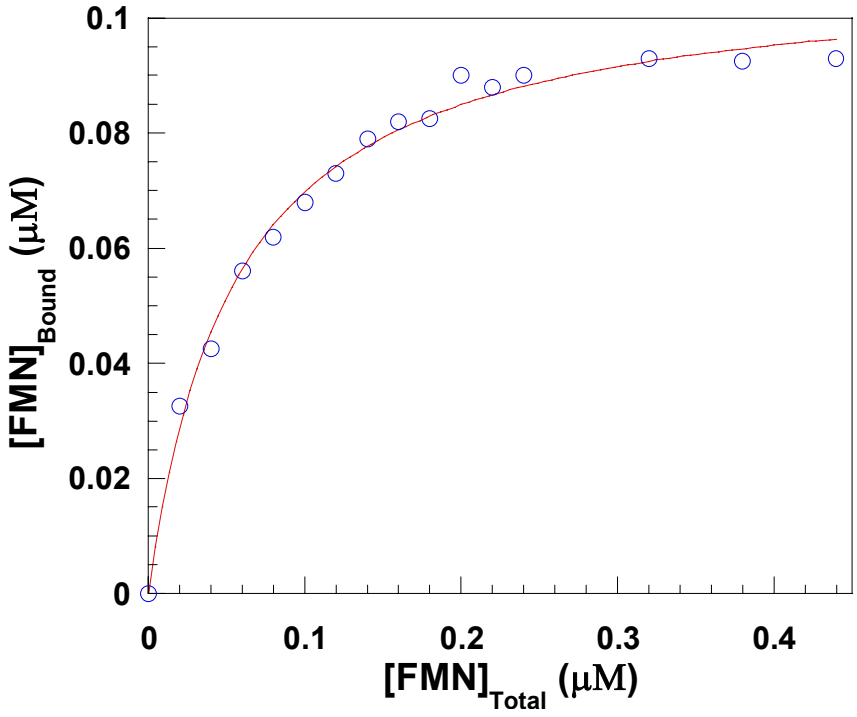

Figure 4.7. Determination of the K_d of wild type SsuE. Proteine concentration was 0.1 μM, FMN concentration was from 0-0.5 μM (37).

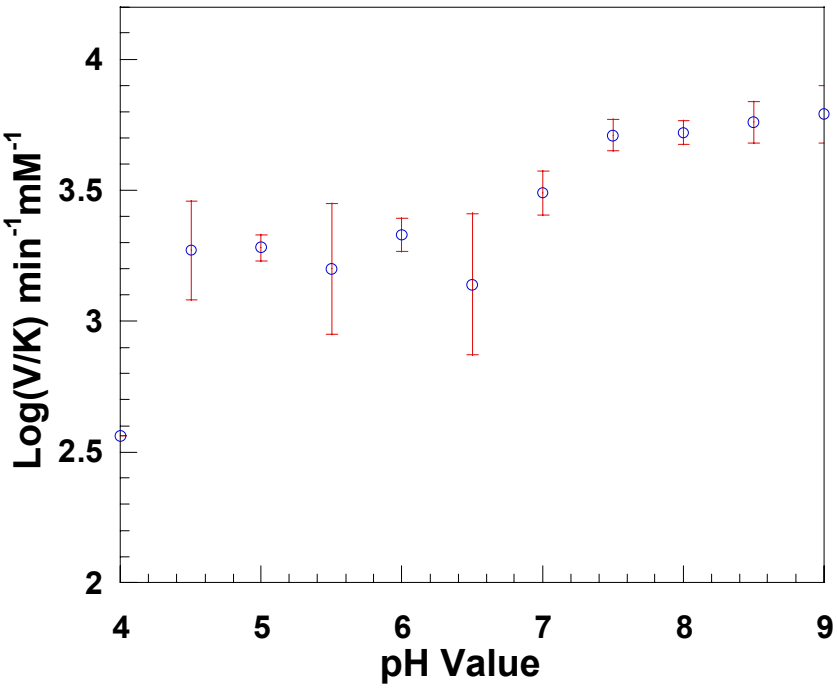

Figure 4.8. The pH dependence of *V*/*K* value for wild type SsuE. Protein concentration was 0.05 μM, NADPH concentration was 120 and FMN concentration was 0.2 μM.

4.4 Discussion

4.4.1 Kinetic studies of S54A and F52A SsuE

The steady-state kinetic analysis of wild type SsuE has been determined (32). SsuE catalyzes reduction of FMN following an ordered-sequential mechanism in which NADPH binds to SsuE first and $NADP^+$ is released as the final product. Compared with wild type SsuE, the K_m value for S54A SsuE was increased by 5-fold. This suggests that S54A SsuE requires more substrate to reach the same reaction velocity as wild type. The K_d and K_m values were similar to each other for both S54A and wild type SsuE suggesting k_3 is relatively small compared to the value of k_1. Thus, the K_m value can represent FMN binding, and the increase in the K_m value for S54A SsuE is mainly due to changes in binding affinity. Meanwhile, the catalytic efficiency (k_{cat}/K_m) of S54A SsuE decreased by 6-fold, suggesting that the decrease of the catalytic efficiency was also caused by a loss in binding capacity. Additionally, the K_d (k_2/k_1) value of S54A SsuE was 0.12 μM which was slightly larger than the K_m value (0.09 μM). Because the K_m of S54A SsuE was obtained with NADPH present, the binding of NADPH to SsuE may favor FMN binding.

For F52A SsuE, the K_m value was increased by 18-fold and K_d was increased by 3-fold compared with wild type SsuE. The increase in the K_m value is 6 times larger than the corresponding increase in the K_d value, and the catalytic efficiency of F52A SsuE was

decreased by 24-fold compared to wild type SsuE. The increase in K_m value may be caused by alterations in the active site, suggesting Phe52 is directly involved in FMN catalysis.

4.4.2 pH profile of SsuE

A common measure of enzyme substrate specificity is the V/K value. Kinetically the V/K value is the second order rate constant for the reaction of free enzyme and substrate to form the first committed species (43). As scheme 4.1 **B** shows, V/K value represents $k_1k_3/(k_2+k_3)$. Thus the V/K value is a combination of rate constants reflecting both binding (k_1,k_2) and catalysis (k_3). The change in the V/K value with increasing pH could be due to FMN binding or direct catalysis. The pH profile of enzymes utilizing acid/base catalysis is often bell-shaped. In such examples an acidic residue with a low pK_a must be unprotonated while a basic residue with a high pK_a must be protonated.

The pH profile of SsuE showed that SsuE activity had a dependence on pH. However, the data could not be fitted to any of the appropriate equations (41-42). When the pH was altered from 4.0 to 5.0, the activity of SsuE increased about 10-fold. Thus, a residue with a pK_a between 4.0~5.0 was likely unprotonated within the active site. According to studies of the FNR family, the conserved residue Asp53 of SsuE may be involved in

catalysis. In the FNR family, this Asp residue forms a hydrogen bond to the catalytically important serine, and replacement of this residue with alanine leads to a significant decrease in the electron-transfer rate between FNR and its substrates (37). This residue has been proposed to participate in proton transfer coupled to electron transfer during catalysis (35-36). Although there was no precipitation in the control experiment for CDO under low pH, the folding stability of SsuE might be affected at low pH values leading to a decrease in catalytic activity.

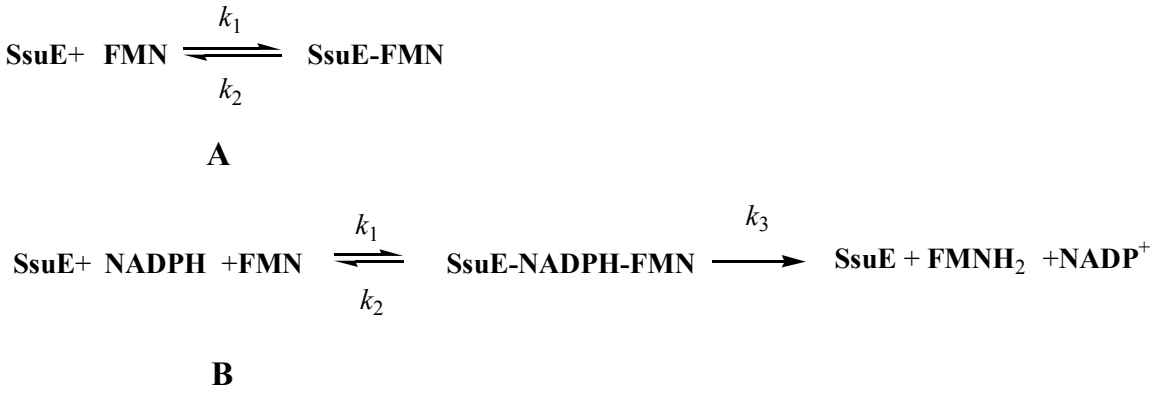

Scheme 4.1. Reactions involved in the kinetic study of S54A, F52A, and wild type SsuE.

Table 4.1 Steady-state kinetic parameters for FMN to bindS54A, F52A, and wild type SsuE

	K_m (μM)	K_{cat} (min^{-1})	K_d (μM)	K_{cat}/K_m ($\mu M^{-1} \cdot min^{-1}$)
Wild type SsuE	0.016	116.0	0.015	7250.0
SsuES54A	0.09	101.83	0.12	1131.44
SsuEF52A	0.30	90.04	0.049	300.1

4.5 Summary

In conclusion, CDO and SsuE/SsuD both utilize sulfur containing substrates and provide sulfur sources for the cell. CDO is mainly involved in cysteine metabolism in mammalian systems, while SsuD/SsuE utilizes organic sulfur substrates when bacteria are under sulfur starvation conditions.

Rat CDO protein without a His tag has been expressed and purified from *E. coli*. The CDO protein from the cell pellet separated as one band on SDS-PAGE, however, two bands were observed at the end of the purification. Corresponding to the decrease of the upper molecular weight band, the activity of CDO decreased until it was no longer detectable. The two bands of CDO from SDS-PAGE were separated, and the results showed that these two bands were both CDO protein with similar molecular weights and amino acid sequences. The three-dimensional crystal structure of CDO revealed a Tyr157-Cys93 covalent crosslink near the Fe center of the active site (Figure 3.7). This crosslink is likely responsible for the activity loss and the presence of the lower band on SDS-PAGE.

EPR studies of CDO with and without cysteine showed that the g-values changed from 4.36 to 4.44 respectively. In addition, the intensity of CDO signal with cysteine is higher than that without cysteine. These results suggested that cysteine incubation altered the environment of the iron center. Future studies will focus on the role of the

Tyr157-Cys93 crosslink and the identification the binding of cysteine to CDO protein.

The amino acid substitution of Phe52 and Ser54 to Ala has been performed based on the conserved RXXS motif, which was observed in the FNR family and SsuE. The proteins, S54A and F52A SsuE, were expressed and purified from *E. coli*. Kinetic studies of S54A SsuE showed that the K_d value of S54A SsuE was increased by 8-fold and k_{cat}/K_m value by 6-fold compared with wild type SsuE. These data suggest that Ser54 is involved in flavin binding. The k_{cat}/K_m value of F52A SsuE was decreased by 24-fold and the K_d value increased by 3-fold compared to wild type SsuE. This change in the kinetic parameters suggests Phe52 may be involved in FMN reduction rather than flavin binding. The optimal activity for SsuE occurs above pH 5.0.

REFERENCES

1. J. R. van der Ploeg, E. Eichhorn, and T. Leisinger, Sulfonate-sulfur metabolism and its regulation in *Escherichia coli, Arch Microbiol* 176 (2001) 1-8.

2. D. L. Bella, L. L. Hirschberger, Y. Hosokawa, and M. H. Stipanuk, Mechanisms involved in the regulation of key enzymes of cysteine metabolism in rat liver in vivo, *Am J Physiol.* 276 (1999) 326-335.

3. S. C. Chai, A. A. Jerkins, J. J. Banik, I. Shalev, J. L. Pinkham, P. C. Uden, and M. J. Maroney, Heterologous expression, purification, and characterization of recombinant rat cysteine dioxygenase, *The Journal of Biochemical Chemistry* 280 (2005) 9865-9869.

4. Y. H. Kwon, and M. H. Stipanuk, Cysteine regulates expression of cysteine dioxygenase and γ-glutamylcysteine synthetase in cultured rat hepatocytes, *Am J Physiol Endocrinol Metab* 280 (2001) 804-E815.

5. E. Erichhorn, J. R. van der Ploeg, and T. Leisinger, Characaterization of a two-component alkanesulfonate monooxygenase from *Escherichia coli*, *The Journal of Biochemical Chemistry* 274 (1999) 26639-26646.

6. A. Kahnert, P. Vermeij, C. Wietek, P. James, T. Leisinger, and M. A. Kertesz, The *ssu* locus plays a key role in organosulfur metabolism in *Pseudomonas putia* S-313, *Journal of Bacteriology* 182 (2000) 2869-2878.

7. L. J. Wilkinson, and R. H. Waring, Cysteine dioxygenase: modulation of expression in human cell lines by cytokines and control of sulphate production, *Toxicology in Vitro* 16 (2002) 481-483.

8. S. H. Hansen, The role of taurine in diabetes and the development of diabetic complications, Diabetes *Metab Res Rev* (2001), 330-346.

9. S. Sakakibara, K. Yamaguchi, Y. Hosokawa, N. Kohashi, and I. Ueda (1976) *Biochim.*

Biophys. Acta 422 (1976) 273–279.

10. D. Voet, and J. G. Voet, *Biochemistry*, Second edition, 338.

11. M. H. Stipanuk, L. L. Hirschberger, M. P. Londono, C. L. Cresenzi, and A. F. Yu, The ubiquitin-proteasome system is responsible for cysteine-responsive regulation of cysteine dioxygenase concentration in liver, *Am J Physiol Endocrinol Metab* 286 (2004) 439-448.

12. J. E. Dominy Jr, L. L. Hirschberger, R. M. Coloso and M. H. Stipanuk, Regulation of cysteine dioxygenase degradation is mediated by intracellular cysteine levels and the ubiquitin-26 S proteasome system in the living rat, *Biochem. J.* 394 (2006) 267-273.

13. R. H. Garrett, and C. M. Grisham, *Biochemistry*, 2nd edition (1999), 1122-1125.

14. Y. Hosokawa, A. Matsumoto, J. Oka, H. Itakura, and K. Yamaguchi, Isolation and characterization of a cDNA from rat liver cysteine dioxygenase, *Biochemical and Biophysical Communications* 168 (1990) 473-478.

15. L. Wang, D. J. Thiel, C. Hickey, L. L. Hirschberger, M. Londono, and M. H. Stipanuk, Evidence for expression of a single distinct form of mammalian cysteine dioxygenase, *Amino Acids* 26 (2004) 99-106.

16. B. Sörbo, and L. Ewetz, The enzymatic oxidation of cysteine to cysteinesulfinate in rat liver, *Biochem Biophys. Res. Commun.* 18 (1965) 359.

17. J. B. Lombardini, and T. P. Singer, Cysteine oxygenase II. Study on the mechanism of the reaction with ^{18}Oxygen, *The Journal of Biological Chemistry* 244 (1969) 1172-1175.

18. O. Hayaishi, T. P. Singer, Biological oxidations, *Interscience Publishers*, New York (1968), 581.

19. M. Costas, M. P. Mehn, M. P. Jensen, and L. Que, Dioxygen activation at mononuclear nonheme iron active sites: enzymes, models, and intermediates, *Chem. Rev.* 104 (2004), 939 -986.

20. L. Que, One motif- many different reactions, *Nat. Struct. Biol.* 7 (2000) 182-185.

21. E. I. Solomon, T. C. Brunold, M. I. Davis, J. N. Kemsley, S. Lee, N. Lehnert, F. Neese, A. J. Skulan, Y. Yang, and J. Zhou, *Chem. Rev.* 100 (2000) 235.

22. R. H. Holm, P. Kennepohl, and E. I. Solomon, Structural and functional aspects of metal sites in biology, *Chem. Rev.* 96 (1996) 2239-2314.

23. J. G. McCoy, L. J. Bailey, E. Bitto, C. A. Bingman, D. J. Aceti, B. G. Fox, and G. N. Philips, Jr , Structure and mechanism of mouse cysteine dioxygenase, *PNAS* 103 (2006) 3084-3089.

24. C. R. Simmons, Q. Liu, Q. Huang, Q. Hao, T. P. Begley, P. A. Karplus, and M. H. Stipanuk , *JBC* in press (2006).

25. E. Eichhorn, C. A. Davey, D. F. Sargent, T. Leisinger, and T. J. Richmond, Crystal structure of *Escherichia coli* alkanesulfonate monooxygenase SsuD, *J. Mol. Biol.* 324 (2002) 457-468.

26. N. M. Kredich, In *Escherichia coli* and salmonella: cellular and molecular biology, *American Society for Microbiology Washington, D. C.* (1996), 514-527.

27. J. R. van der Ploeg, R. Iwanicka-Nowicka, T. Bykowski, M. M. Hryniewicz, and T. Leisinger, The *Escherichia coli* ssuEADCB gene cluster is required for the utilization of sulfur from aliphatic sulfonates and is regulated by the transcriptional activator Cbl, *The Journal of Biological Chemistry* 274 (1999) 29358-29365.

28. M. A. Kertesz, K. Schimidt-Larbig, and T. Wüest, A novel reduced flavin mononucleotide-dependent methanesulfonate sulfonatase encoded by the sulfur-regulated *msu* operon of P*seudomonas aeruginosa*, *J. Bacteriol.* 181 (1999) 1464-1473.

29. C. F. Higgins, ABC transporters: from microorganisms to man, *Annu. Rev. Cell Biol.* 8 (1992) 67-113.

30. M. Wistchel, S. Nagel, and T. Egli, Identification and characterization of the two-enzyme system catalyzing oxidation of EDTA in the EDTA-degrading bacterial strain DSM 9103, *J. Bacteriol.* 179 (1997) 6937-6943.

31. L. Xi, C. H. Squires, D. J. Monticello, and J. D. Childs, A flavin reductase stimulates DszA and DszC proteins of *Rhodococcus erythropolis*IGTS8 in vitro, *Biochem. Biophys. Res. Commun.* 230 (1997) 73-75.

32. B. Gao, and H. R. Ellis, Altered mechanism of the alkaesulfonate FMN reductase with the monooxygenase enzyme, *Biochemical and Biophysical Research*

Communications 331 (2005) 1137-1145.

33. D. F. Becker, U. Leartsakulpanich, K. K. Surerus, J. G. Ferry, and S. W. Ragsdale, Electrochemical and spectroscopic properties of the iron-sulfur flavoprotein from *methanosarcina thermophila*, *J. Biol. Chem.* 273 (1998) 26462-26469.

34. F. Fieschi, V. Nivièrei, C. Frier, J.-L. Décout, and M. Fontecave, The mechanism and substrate specificity of the NADPH:flavin oxidoreductase from *Escherichia coli*, *J. Biol. Chem.* 270 (1995) 30392-30400.

35. V. Nivièrei, F. Fieschi, J.-L. Décout, and M. Fontecave, Is the NAD(P)H:Flavin oxidoreductase from *Escherichia coli* a member of the ferredoxin-$NADP^+$ reductase family?, *The Journal of Biological Chemistry* 271 (1996) 16656-16661.

36. M. Ingelman, S. Ramaswamy, V. Nivièrei, M. Fontecave, and H. Eklund, Crystal structure of NAD(P)H:flavin oxidoreductase from *Escherichia coli*, *Biochemistry* 38 (1999) 7040-7049.

37. M. Medina, M. Marinez-Julvez, J. Hurley, G. Tollin, and C. Gomez-Moreno, *Biochemistry* 37 (1998) 2715-2728.

38. A. Kantz, F. Chin, N. Nalamothu, T. Nguyen, and G. T. Gassner, Mechanism of flavin transfer and oxygen activation by the two-component flavoenzyme styrene monooxygenase, *Archives of Biochemistry and Biophysics* 442 (2005) 102-116.

39. B. Lei, and S.-C. Tu, Mechanism of reduced flavin transfer from *Vibrio harveyi* NADPH-FMN oxidoreductase to luciferase, *Biochemistry* 37 (1999) 14623-14629.

40. T. M. Louie, X. S. Xie and L. Xun, Coordinated production and utilization of $FADH_2$ by NAD(P)H-flavin oxidoreductase and 4-hydroxyphenylacetate 3-monooxygenase, *Biochemistry* 42 (2003), 7509–7517.

41. G. Gadda, pH and deuterium kinetic isotope effects studies on the oxidation of choline to betaine-aldehyde catalyzed by choline oxidase, *Biochimica et Biophysica Acta* 1650 (2003), 4-9.

42. G. Gadda, and P. F. Fitzpatrick, Mechanism of nitroalkane oxidase: 2. pH and kinetic isotope effects, *Biochemistry* 39 (2000), 1406-1410.

43. G. Gadda, D. Y. Choe, and P. F. Fitzpatrick, Use of pH and kinetic isotope effects to dissect the effects of substrates size on binding and catalysis by nitroalkane oxidase,

Archives of Biochemistry and Biophysics (2000), Vol. 382, No. 1, 138-144.

44. K. P. McCann, M. T. Akbari, A. C. Williams, and D. B. Ramsden, Human cysteone dioxygenase type I: primary structure derived from base sequence of cDNA, *Biochimica et Biophysica Acta* 1209 (1994), 107-110

45. M. Quadroni, W. Staudenmann, M. Kertesz, and P. James, Analysis of global response by protein and peptide fingerprinting of proteins isolated by two-dimensional gel electrophoresis, *Eur. J. Biochem* 239 (1996), 773-781

46. J. R. Van der Ploeg, M. A. Weiss, E. Saller, H. Nashimoto, N. Saito, M. A. Kertesz, and T. Leisinger, Identification of sulfate starvation-regulated genes in *Escherichia coli*: a gene cluster involved in the utilization of taurine as a sulfur source, *Journal of Bacteriology* (1996) 5438-5446

47. D. L. Nelson, and M. M. Cox, *Principles of biochemistry fourth edition* (2005) 225-233